

# The Helium abundance and $\Delta Y/\Delta Z$ in Lower Main Sequence stars

Luca Casagrande<sup>1,2</sup>, Chris Flynn<sup>1,2</sup>, Laura Portinari<sup>1,2</sup>, Leo Girardi<sup>3</sup>, Raul Jimenez<sup>4</sup>

<sup>1</sup> Tuorla Observatory, Department of Physics, University of Turku, Väisäläntie 20, FIN-21500, Piikkiö, Finland

<sup>2</sup> Department of Physics, University of Turku, FIN-20014 Turku, Finland

<sup>3</sup> Osservatorio Astronomico di Padova, Vicolo dell’Osservatorio 5, 35122 Padova, Italy

<sup>4</sup> Department of Physics and Astronomy, University of Pennsylvania, PA 19104, USA

6 November 2018

## ABSTRACT

We use nearby K dwarf stars to measure the helium-to-metal enrichment ratio  $\Delta Y/\Delta Z$ , a diagnostic of the chemical history of the Solar Neighbourhood. Our sample of K dwarfs has homogeneously determined effective temperatures, bolometric luminosities and metallicities, allowing us to fit each star to the appropriate stellar isochrone and determine its helium content indirectly. We use a newly computed set of Padova isochrones which cover a wide range of helium and metal content.

Our theoretical isochrones have been checked against a congruous set of main sequence binaries with accurately measured masses, to discuss and validate their range of applicability. We find that the stellar masses deduced from the isochrones are usually in excellent agreement with empirical measurements. Good agreement is also found with empirical mass-luminosity relations.

Despite fitting the masses of the stars very well, we find that anomalously low helium content (lower than primordial helium) is required to fit the luminosities and temperatures of the metal poor K dwarfs, while more conventional values of the helium content are derived for the stars around solar metallicity.

We have investigated the effect of diffusion in stellar models and LTE assumption in deriving metallicities. Neither of these is able to resolve the low helium problem alone and only marginally if the cumulated effects are included, unless we assume a mixing-length which is strongly decreasing with metallicity. Further work in stellar models is urgently needed.

The helium-to-metal enrichment ratio is found to be  $\Delta Y/\Delta Z = 2.2 \pm 1.1$  around and above solar metallicity, consistent with previous studies, whereas open problems still remain at the lowest metallicities. Finally, we determine the helium content for a set of planetary host stars.

**Key words:** stars: Hertzsprung-Russell (HR) diagram – stars: abundances – stars : late-type – stars: interiors – stars: colours, luminosities, masses, radii, temperatures, etc. – binaries: general

## 1 INTRODUCTION

K dwarfs can be regarded as snapshots of the stellar populations formed at different times over the history of our Galaxy, and therefore constitute an optimal tool for any study dealing with its chemical evolution (e.g. Kotoneva et al. 2002). The helium abundance in such objects determines their lifetime, luminosity and internal structure and thus links their physical properties to important astrophysical considerations regarding nucleosynthesis and chemical evolution studies. The initial helium abundance  $Y$  of stars born in different sites, with different metallicities  $Z$  and plausibly

different physical conditions tells us much about the processes of star formation and evolution. The ratio  $\Delta Y/\Delta Z$  is thus a valuable diagnostic to characterize the evolution of stellar populations in galaxies. Age determinations of both resolved and integrated stellar populations rely on knowing their helium content as a function of metallicity and accurately knowing the age of galaxies can, in turn, help to determine the nature of dark energy (Jimenez & Loeb 2002). Metals mainly come from massive stars undergoing supernova explosions whereas helium is also produced by mass-loss from intermediate and low mass stars : the ra-

tio  $\Delta Y/\Delta Z$  can thus be predicted from stellar evolutionary theory once a certain initial mass function is assumed (e.g. Chiosi & Matteucci 1982; Maeder 1992, 1993; Chiappini, Renda & Matteucci 2002). The ratio  $\Delta Y/\Delta Z$  is also useful to infer the primordial helium abundance  $Y_P$  by extrapolating to  $Z = 0$ . This technique is usually applied to extragalactic H II regions; Cosmic Microwave Background measurements alone are not able to provide a tight constraint in  $Y_P$  (Trotta & Hansen, 2004), yet WMAP3 data on the cosmic baryon density when combined with Standard Big Bang Nucleosynthesis return a formally accurate value for  $Y_P$  (see Section 4.2).

Helium lines are not easily detectable in the spectra of low mass stars, apart from the case of hot horizontal branch objects, whose atmospheres are, however, affected by gravitational settling and radiative levitation, which strongly alter the initial chemical stratification (e.g. Michaud, Vauclair & Vauclair 1983, Moehler et al. 1999) and whose composition anyway would not reflect the original helium abundance at their birth. Therefore, assumptions have to be made for the initial helium content of models of low-mass stars. Very often it is supposed that the metallicity  $Z$  and helium fraction  $Y$  are related through a constant ratio  $\Delta Y/\Delta Z$ . The latter is often determined from the result of the solar calibration  $(Y_\odot - Y_P)/Z_\odot$  and for any other star of known metallicity, the helium abundance is scaled to the solar one as  $Y = Y_\odot + \frac{\Delta Y}{\Delta Z} \times (Z - Z_\odot)$ . Most of the conclusions drawn when comparing theoretical isochrones with binaries (e.g. Torres et al. 2002; Torres & Ribas 2002; Lacy et al. 2005; Torres et al. 2006; Boden, Torres & Latham 2006; Henry et al. 2006) and field stars (e.g. Allende Prieto & Lambert 1999; Valenti & Fischer 2005) thus reflect this tacit assumption on the helium content.

Recent results, however suggest that the naive assumption that  $\Delta Y/\Delta Z$  varies linearly and with a universal law might not be correct. For example, the Hyades seem to be  $Y$  deficient for their metallicity (Perryman et al. 1998; Lebreton, Fernandes & Lejeune 2001; Pinsonneault et al. 2003). The discovery that the Globular Cluster  $\omega$  Cen has at least two different components of the Main Sequence and multiple turnoffs (Lee et al. 1999; Pancino et al. 2000, 2002; Ferraro et al. 2004; Bedin et al. 2004) can be explained assuming stellar populations with very different helium abundances (Norris 2004). Recently, compelling evidence has been found for a helium spread among the Main Sequence in the Globular Clusters NGC 2808 (D'Antona et al. 2005a) and the blue horizontal branch stars in the Globular Cluster NGC 6441 (Caloi & D'Antona 2007). At the same time, for a different sample of Galactic Globular Clusters Salaris et al. (2004) found a very homogeneous value of  $Y$  with practically no helium abundance evolution over the entire metallicity range spanned by their study. All this suggests that a patchy variation of  $\Delta Y/\Delta Z$  and complex chemical evolution histories might be not so unusual in our Galaxy. Similar indications also start to appear for extragalactic objects (Kaviraj et al. 2007). There are various methods to infer the helium content in Globular Clusters (e.g. Sandquist 2000) and all take advantage of the fact that in these objects it is relatively easy to perform statistical analysis over large stellar populations.

The determination of the helium content in nearby field stars, on the contrary, is more challenging, because it is not so straightforward to build a statistically large and homo-

geneously selected sample. Accurate parallaxes are needed and to avoid subtle reddening corrections only stars closer than  $\sim 50 - 70$  pc must be used. All studies to date have exploited the fact that the broadening of the Lower Main Sequence with metallicity effectively depends on the helium content (see Section 4) so that its width can be used to put constraints on  $\Delta Y/\Delta Z$  (e.g. Faulkner 1967; Perrin et al. 1977; Fernandes, Lebreton & Baglin 1996; Pagel & Portinari 1998; Jimenez et al. 2003). In this work we take the same strategy, comparing the positions of a large sample of field stars with theoretical isochrones in the  $M_{Bol} - T_{eff}$  plane. For the parameter space covered by the isochrones, the number of stars used, the accuracy and the homogeneity of the observational data (crucial when it comes to analyzing small differential effects in the HR diagram), this is the most extensive and stringent test on the helium content of lower main sequence stars undertaken to date.

An analogous work was pioneered by Perrin et al. (1977) with 138 nearby FGK stars but with much less accurate fundamental stellar parameters, pre-*Hipparcos* parallaxes and of course, older stellar models. After *Hipparcos* parallaxes become available, the problem was re-addressed by Lebreton et al. (1999) with a sample of 114 nearby FGK stars in the metallicity range  $-1.0 < [\text{Fe}/\text{H}] < 0.3$ , of which only 33 have  $T_{eff}$  and  $M_{Bol}$  determined directly via the InfraRed Flux Method (IRFM) of Alonso et al. (1995, 1996a). For the remaining stars, temperatures were either recovered via spectroscopic methods or color indices and  $M_{Bol}$  determined from the bolometric corrections of Alonso (1995, 1996b).

We have recently carried out a detailed empirical determination of fundamental stellar parameters via IRFM (Casagrande, Portinari & Flynn 2006) with the specific task of determining the helium content in dwarf stars by comparing them to theoretical isochrones. Our sample is similar in size to previous studies, but i) it has a larger metallicity coverage ii) we have improved the accuracy in the selection (see Section 2), iii) we have carefully and homogeneously determined the fundamental stellar parameters iv) focusing particularly on stars (K dwarfs) where the helium content can be most directly determined from the stellar structure since the effects of stellar evolution have not yet played any role.

Stellar models are common ingredients in a variety of studies addressing fundamental cosmological and astrophysical problems, from ages and evolution of galaxies, to complex stellar populations, to exoplanets. Still, our incomplete understanding of complex physical processes in stellar interior requires the introduction of free parameters that are calibrated to the Sun. Therefore, using main sequence nearby stars with accurate fundamental parameters to test the adequacy of extant stellar models is of paramount importance to validate their range of applicability (Lebreton 2000), as we do here.

The paper is organized as follows. In Section 2 we describe our sample and in Section 3 we present our theoretical isochrones and how they compare to observations. In Section 4 we delve into the derivation of the helium abundance for Lower Main Sequence stars and in Section 5 we carefully analyze how the results depend on the assumptions made in stellar models. The applicability range of our results is obtained by comparing the prediction of the isochrones to a congruous set of Main Sequence binaries (Section 6) and to

empirical mass-luminosity relations (Section 7). We suggest that an accurate mass-luminosity relation for metal poor dwarfs could actually put constraints on their helium content. In Section 8 we apply our method to derive masses and helium abundances for a small set of planet host stars. We finally conclude in Section 9.

## 2 SAMPLE AND DATA SELECTION

Our sample stems from the 104 GK dwarfs for which we computed accurate effective temperatures and bolometric luminosities via Infra-red Flux Method (hereafter IRFM — Casagrande et al. 2006). For such stars accurate overall metallicities [M/H] are also available from spectroscopy<sup>1</sup>. This is a very important point when data are compared to stellar models: neglecting the  $\alpha$  enhancement can in fact lead to erroneous or biased conclusions (Gallart, Zoccali & Aparicio 2005). We also paid special attention to remove unresolved double/multiple and variable stars as described in more details in Casagrande et al. (2006).

Some of the stars in the sample were too bright to have accurate 2MASS photometry and therefore the IRFM could not be applied. However, such stars have excellent  $BV(RI)_C$  photometry so that from these colours it was possible to recover the effective temperature and bolometric flux by means of the multi-band calibrations given in Casagrande et al. (2006), homogeneously with the rest of the sample. In this manner twenty-three single (or well separated binary) and non variable stars were added to the sample. For these additional stars  $T_{eff}$  and  $\mathcal{F}_{Bol}(\text{earth})$  have been estimated averaging the values returned by the calibrations in all  $BV(RI)_C$  bands. The standard deviation resulting from the values obtained in different bands has been adopted as a measure of the internal accuracy. The systematics due to the adopted absolute calibration (Figure 12 in Casagrande et al. 2006) have then been added to obtain the overall errors. When helium abundances for these additional stars are computed (Section 4), the resulting values are perfectly in line with those obtained for stars with fundamental parameters obtained via IRFM.

We remark that an accurate estimate of the absolute luminosity (or magnitude) of each star requires parallax accuracy at the level of a few percent. A possible limitation could be the Lutz-Kelker (1973) bias. However, as we discuss in Appendix A, when limiting our sample to parallaxes better than 6% the bias is negligible compared to other uncertainties. This requirement on the parallaxes reduces our sample to 105 stars (see Figure 1).

We derive the helium content of our stars by comparing their positions in the theoretical HR diagram with respect to a set of isochrones of different helium and metallicity content (see Section 4). If evolutionary effects have already taken place in stars, the comparison would be age dependent (see Section 3). However, for any reasonable assumption about

<sup>1</sup> The best measured elemental abundance in dwarf stars is usually iron (i.e. [Fe/H]) whereas for theoretical models the main metallicity parameter is the total heavy-element mass fraction [M/H]. For our stars  $Z = Z_{\odot} \times 10^{[\text{M}/\text{H}]}$  has been obtained from detailed spectroscopic composition and  $[\alpha/\text{Fe}]$  ratios as described in Casagrande et al. (2006)

the stellar ages, one can safely assume that all stars fainter than  $M_V \sim 5.5$  are practically unaffected by evolution and lie close to their Zero Age Main Sequence (ZAMS) location (e.g. Fernandes et al. 1996; Pagel & Portinari 1998; Jimenez et al. 2003). In terms of  $M_{Bol}$  the threshold is very similar (see figure 17 in Casagrande et al. 2006) so that we assume  $M_{Bol} \geq 5.4$  as a conservative estimate : this reduces the sample to 86 K dwarfs.

For consistency with Casagrande et al. (2006), throughout the paper we assume  $M_{Bol,\odot} = 4.74$  and  $L_{\odot} = 3.842 \times 10^{33} \text{ erg s}^{-1}$ .

## 3 THEORY

### 3.1 Fine structure in the HR diagram: the broadening of the Lower Main Sequence

Several effects are responsible for the observed width of the Main Sequence : among the physical ones are chemical composition, evolution and rotation whereas observational errors and undetected binarity among stars are spurious ones. We have carefully cleaned our sample from spurious effects (Casagrande et al. 2006) so here we discuss only the physical ones related to stellar structure.

The cut in absolute magnitudes adopted for our sample (Section 2) ensures that our stars have masses below solar. The location of the Main Sequence depends on the treatment of convection and the size of core convective regions only for stars with  $M > 1.1M_{\odot}$  and on rotation for stars with  $M > 1.4M_{\odot}$  (e.g. Fernandes et al. 1996) so these effects and the related theoretical uncertainties are of no concern to us.

With typical masses  $\sim 0.8M_{\odot}$  K dwarfs have lifetimes longer than the present age of the Galactic disk (e.g. Jimenez, Flynn & Kotoneva, 1998) and comparable to the present age of the Universe (Spergel et al. 2006) so that their temperature and bolometric luminosity are insensitive to the stellar age and depend exclusively on their mass, helium content ( $Y$ ) and metallicity ( $Z$ ). For a given metallicity  $Z$ , an increase of  $Y$  makes a given mass on the isochrone hotter and brighter so that the net result of varying  $\Delta Y/\Delta Z$  is to affect the broadening of the Lower Main Sequence (see Figures 1 and 2). Such a behaviour can be explained in terms of quasi-homology relations (an increase of  $Y$  in fact decreases the mean opacity and increases the mean molecular weight e.g. Cox & Giuli 1968; Fernandes et al. 1996) and it has been exploited by Pagel & Portinari (1998) and more recently by Jimenez et al. (2003) to put constraints on the local  $\Delta Y/\Delta Z$ .

### 3.2 Evolutionary tracks and isochrones

We have computed a series of stellar models, using the Padova code as in Salasnich et al. (2000). Since our sample includes only dwarfs, the evolutionary tracks are limited to the Main Sequence phase only. We consider a range of metallicities from  $Z = 0.0001$  to  $Z = 0.04$ , and a range of  $\Delta Y/\Delta Z$  between 0 and 6. Metal abundance ratios are taken from Grevesse & Noels (1993). The solar metallicity is fixed to be  $Z_{\odot} = 0.017$ , which is the value preferred by Bertelli et al. (2007, in prep.) to whom we refer for all details. With this  $Z_{\odot}$ , the model that reproduces the present

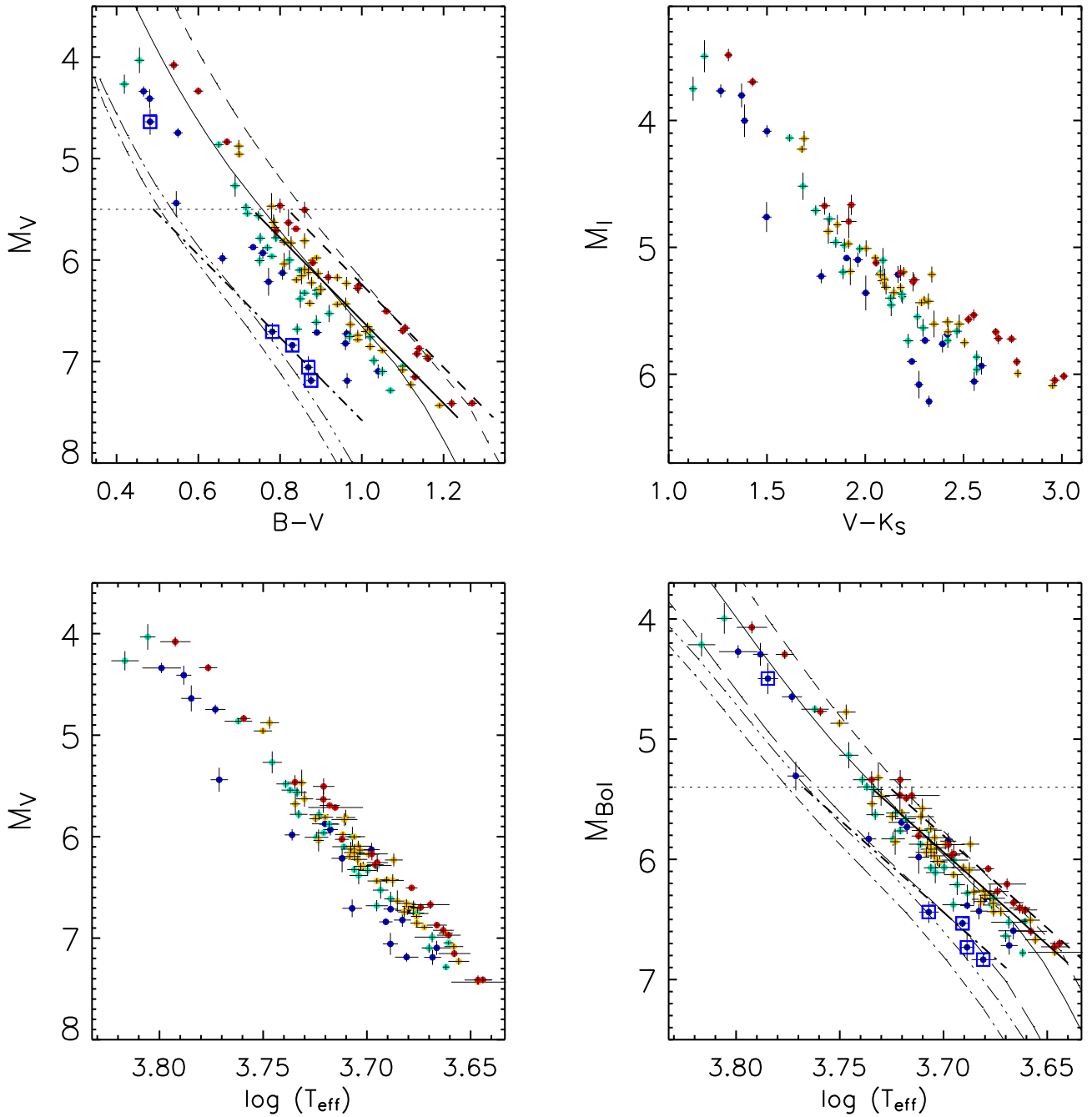


**Figure 1.** Comparison between observational, hybrid and theoretical planes. Parallax uncertainties are also included in error bars. Only stars with parallaxes better than 6% are shown. For the second panel ( $M_I, (V - K_S)$ ) only stars with accurate IR photometry (“j\_”+“h\_”+“k\_msigcom”< 0.10) are shown. Points correspond to the sample stars in the range  $Z < 0.006$  (blue),  $0.006 \leq Z < 0.012$  (cyan),  $0.012 \leq Z < 0.022$  (yellow),  $Z \geq 0.022$  (red). Squares are intended to highlight stars with  $0.0007 \leq Z \leq 0.0013$  to facilitate comparison with metal poor isochrones. Overplotted are 1 Gyr isochrones of metallicity  $Z = 0.001$  (dot dashed),  $0.017$  (continuous) and  $0.040$  (dashed) under the standard assumption of  $\Delta Y / \Delta Z = 2$ . The lower and upper  $Z$  value roughly bracket the metallicity of our sample. Also shown for comparison (triple dot dashed) is an extremely helium poor isochrone ( $Z = 0.001$  and  $Y = 0.167$ ). In the fourth panel is also plotted an isochrone with  $Z = 0.004$  and  $Y = 0.250$  (long dashed line). Thick lines are empirical fits to the stars plotted for the same metallicity ( $Z = 0.001, 0.017, 0.040$ ) as the isochrones (see Section 3.3).

solar radius and luminosity at an age of 4.6 Gyr was found to have  $Y_{\odot} = 0.263$ , and  $\alpha_{MLT} = 1.68$ . These numbers imply  $(Z/X)_{\odot} = 0.0236$  which is slightly below the 0.0245 ratio quoted by Grevesse & Noels (1993) themselves. However, our choice is to have a solar model that fits well the solar position in the HR diagram, and is by no means intended to be an accurate re-calibration. As we will see later, small errors in this calibration procedure, and especially in  $Y_{\odot}$ , are unlikely to affect our results. We also remark that the solar model is presently under profound revision after the updates in the estimated solar abundances (Asplund, Grevesse & Sauval, 2005) significantly diminish the agreement with helioseismology (e.g. Basu & Antia 2004; Antia & Basu 2005). The present study however refers the “classic” solar model and metallicity as the zero-point calibration, and since the method relies on differential effects along the Main Sequence we do not expect that conclusions on  $\Delta Y / \Delta Z$ , which is a *differential* quantity, are significantly affected. Also, as already pointed out, the solar zero-point should be regarded as a calibration parameter and not as an absolutely determined value so that strong inferences on *absolute* values (among which  $Y_P$ ) can hardly be drawn.

The tracks computed cover the mass range between 0.15 and  $1.5 M_{\odot}$ , which is far wider than needed for an analysis of our sample. Regarding convection, we adopt the same prescription as in Girardi et al. (2000): convective core overshooting is assumed to occur for stars with  $M > 1.0 M_{\odot}$ , with an efficiency  $\Lambda_c = M/M_{\odot} - 1.0$  (see Bressan et al. 1993 for the definition of  $\Lambda_c$ ) that increases linearly with mass in the interval from 1 to  $1.5 M_{\odot}$ . Lower mass stars are computed assuming the classical Schwarzschild criterion.

From these tracks, we can construct isochrones in the HR diagram for arbitrary ages, and any intermediate  $Y(Z)$  relation, via simple linear interpolations within the grid of tracks.

Although our analysis is conducted using Padova isochrones, we have fully cross checked (Section 4) the results with an updated set of the MacDonald isochrones (Jimenez & MacDonald 1996; Jimenez et al. 2003) computed for a similar grid of values in  $Y$  and  $Z$ . We have also compared our isochrones with other sets in the low Main Sequence. Namely, we have used Yonsei-Yale (Demarque et al. 2004) and Teramo (Cordier et al. 2007) isochrones for similar values of  $Y$  and  $Z$ . A detailed comparison is outside the purpose of the paper, but we have found a good agreement between different sets so that our results do not depend significantly on the particular isochrones used.

### 3.3 Observational vs. theoretical plane

The comparison between models and data is usually done in the observational colour – absolute magnitude HR diagram rather than in its theoretical  $T_{eff}$ – $M_{Bol}$  counterpart. However, the observational plane makes use of the information extracted only from a limited part of the entire spectral energy distribution of a star (few thousands of Å in the case of broad band colours). Furthermore, for such a comparison theoretical isochrones have to be converted into colours and magnitudes via model atmospheres, introducing further model dependence and uncertainties (e.g. Weiss & Salaris 1999).

Sometimes the hybrid  $T_{eff}$  – absolute magnitude plane

is used although it has almost the same limitations as the observational one (the computation of absolute magnitudes from stellar models still requires the use of spectral libraries). In addition  $T_{eff}$  is rarely empirically and consistently determined for all the stars, more often depending on the adopted colour-temperature transformation or resulting from a collection of inhomogeneous sources in literature. As a result, a single theoretical isochrone produces different loci in the color-magnitude diagram when different color-temperature relations are applied (e.g. Pinsonneault et al. 2004).

Working in the purely theoretical plane has many advantages. First, it is possible to directly compare observations to physical quantities such as temperature and luminosity (or equivalently  $M_{Bol}$ ) predicted from stellar models. Secondly, for the purpose of this work, the effects of helium are highlighted in the theoretical plane, whereas in the widely used  $(B - V)$  vs  $M_V$  plane they are partly degenerate with the dependence of the colour index on metallicity (Castellani, Degl’Innocenti & Marconi 1999). Up to now, the drawback of working in the theoretical plane was that for a given set of stars, very rarely in literature homogeneous and accurate bolometric corrections and effective temperatures were available for large samples. However, for all our stars we have homogeneously derived  $T_{eff}$  and bolometric luminosity from accurate multi-band photometry and basing on the IRFM (Section 2). In the case of K dwarfs  $\sim 80\%$  of the total luminosity is directly observed so that the dependence on model atmosphere is minimal<sup>2</sup>.

The first feature that appears from the comparison between the observational  $(B - V)$  and the theoretical HR diagram (Figure 1) is how in the  $T_{eff}$ – $M_{Bol}$  plane the separation between metal poor and metal rich stars is not as neat as in the observational  $(B - V)$  counterpart. This was already noticed by Perrin et al. (1977) and Lebreton et al. (1999) and reflects the sensitivity of the  $B, V$  colour indices to metallicity. To ensure this is not an artifact due to our temperature and/or luminosity scale, we also show a plot in the observational  $M_I$  versus  $(V - K_S)$  plane.  $(V - K_S)$  is in fact and excellent temperature indicator with negligible dependence on metallicity and  $M_I$  faithfully traces  $M_{Bol}$  (Casagrande et al. 2006). The reduced separation between metal poor and metal rich stars is confirmed.

To quantify how strong is the effect of metallicity in the  $(B - V)$  plane, we have drawn theoretical isochrones in this plane, too. The transformations to convert theoretical isochrones into the observational plane have been obtained by fitting the following formulae to the stars in Casagrande et al. (2006) (their figure 17):

$$BC = a_0 + a_1 T_{eff} + a_2 T_{eff}^2 + a_3 T_{eff} [M/H] + a_4 [M/H] + a_5 [M/H]^2 \quad (1)$$

<sup>2</sup> We further point out that even if model atmospheres are computed with a standard helium content, the spectral energy distribution is largely insensitive to the helium abundance (e.g. Peterson & Carney 1979; Pinsonneault et al. 2004). A  $\Delta Y \sim 0.10$  in model atmospheres changes synthetic magnitudes by  $\Delta m \sim 0.01$  (Girardi et al. 2007). Our implementation of the IRFM relies on multi-band photometry and uses model atmospheres to estimate the missing flux only to a limited extent (few tens of percent). Our results are thus unaffected by this uncertainty.

where  $BC$  is the bolometric correction (from which  $M_V = M_{Bol} - BC$ ) and:

$$B - V = b_0 + b_1 T_{eff} + b_2 T_{eff}^2 + b_3 T_{eff} [M/H] + b_4 [M/H] + b_5 [M/H]^2. \quad (2)$$

Both transformations are accurate to 0.02 mag and the coefficients are given in Table 1.

With this approach the comparison between isochrones and sample stars in the two planes does not depend on model atmospheres, since we use empirical conversions derived from the same sample stars. Notice though that the empirical conversions of Casagrande et al. (2006) show good agreement with theoretical ones from e.g. Kurucz or MARCS model atmospheres.

For the sample stars we have generated empirical isochrones (thick lines in Figure 1) by fitting the following formula to the data (e.g. Castellani, Degl'Innocenti & Marconi 1999) :

$$M_\zeta = c_0 + c_1 Q + c_2 \log Z + c_3 (\log Z)^2 \quad (3)$$

where  $M_\zeta = M_V$  or  $M_{Bol}$  and  $Q = (B - V)$  or  $\log(T_{eff})$ , respectively. Again, we have considered only stars with parallaxes better than 6% and  $M_V \geq 5.5$ ,  $M_{Bol} \geq 5.4$ . The fit is accurate to  $\sim 0.1$  mag. This is a convenient parameterization but is not necessarily the most appropriate fitting formula. Also, the helium content is our unknown parameter and the formulation given above assumes it is the same in all stars of a given metallicity. Although a reasonable assumption, it is not necessarily the case, especially at lower metallicity (see also Figure 5). The slightly different slope between the empirical and the theoretical isochrones probably reflects these shortcoming in the fit as well as the uneven sampling of stars with luminosity. The bulk of the stars have absolute magnitude circa 6, where the agreement between the slope of empirical and theoretical isochrones is good. The sampling becomes more sparse at bright and faint luminosities (where the theoretical isochrones clearly bend). When the theoretical solar isochrone is compared to a restrict sample of solar metallicity stars, the agreement is however outstanding (Figure 7).

From Figure 2 is clear that for metallicity around and above the solar one, empirical and theoretical isochrones with  $\Delta Y/\Delta Z = 2$  are in overall good agreement. On the contrary, a clear discrepancy appears for metal poor stars where the standard assumption  $\Delta Y/\Delta Z = 2$  returns theoretical isochrones that are too hot.

To achieve a match between theoretical and empirical isochrones at the lowest  $Z$ , we need to decrease the corresponding helium abundance down to  $Y = 0.167$ , much below the primordial value expected from Big Bang nucleosynthesis. Even with such a low helium abundance the discrepancy is persistent in the theoretical plane its effects in the observational plane are much less clear. An alternative to reduced helium in the stars is to use a theoretical isochrone with a more orthodox helium abundance ( $Y = 0.250$ , fourth panel in Figure 1) but with a metallicity ( $Z = 0.004$ ) higher by  $\sim 0.6$  dex (with respect to  $Z = 0.001$ ), a very large change in metallicity content indeed (and discussed in detail in Section 5.3). This comparison qualitatively illustrates the results we discuss in the detailed analysis of Section 4.

## 4 HELIUM ABUNDANCE AND MASS FROM THEORETICAL ISOCHRONES

In the previous Section we have shown that the most suitable place to estimate the effects of the helium content on the low Main Sequence is the theoretical  $T_{eff} - M_{Bol}$  plane. Here we delve into this by fitting to each star the most appropriate isochrone; the metallicity  $Z$  of each star is assigned and we thereby determine its helium content  $Y$ . We thus differ from previous works —by means of different techniques— focused on the overall comparison between theoretical predictions and observations along the Lower Main Sequence (Fernandes et al. 1996; Pagel & Portinari 1998; Lebreton et al. 1999; Jimenez et al. 2003). Our approach also avoids any assumption about the existence of a constant, linear helium-to-metal enrichment rate  $\Delta Y/\Delta Z$ . As we discuss later, such a constant ratio can be defined for metallicity around and above the solar one but at lower metallicity the situation is far less clear and linear.

Our isochrone fitting technique provides simultaneously both the helium content and the mass of the stars. With the obvious exception of the Sun, these two quantities have usually been obtained by calibrating stellar models to few nearby visual binary stars (Fernandes et al. 1998; Lebreton et al. 2001; Fernandes, Morel & Lebreton 2002; Pinsonneault et al. 2003) with particular attention to the  $\alpha$  Cen system (see discussion in Section 5 and 6). Unfortunately, for these binary systems the uncertainties in the fundamental physical parameters required to calibrate stellar models are rather large as compared to the Sun so that in the final set of calibration parameters there is a certain degeneracy. To this respect our approach is much more straightforward since the adjustable parameters ( $Y$  and  $\alpha_{MLT}$ ) are strictly calibrated on the Sun (Figure 7). Such calibrated model is then used to compute a large grid of tracks with different metallicities ( $Z$ ) and helium ( $Y$ ) content from which isochrones are constructed. Our grid is used to deduce helium abundances and masses for field stars and the results are validated checking our procedure with a congruous set of binaries whose masses are empirically measured (Section 6).

### 4.1 Method

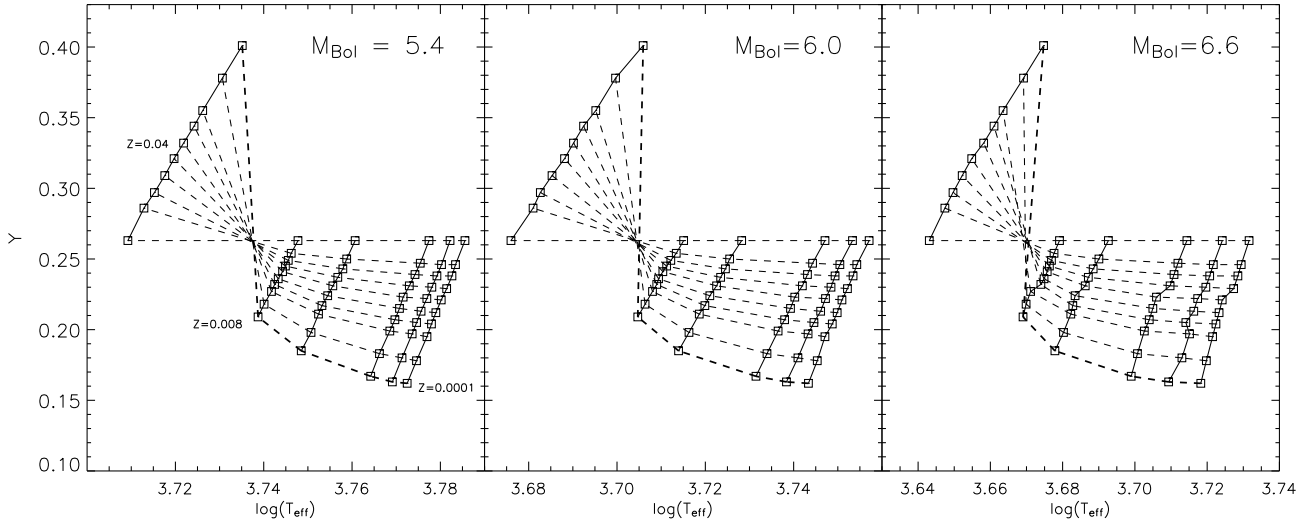
As we have discussed in Section 3 at any given  $M_{Bol}$ , for a given metallicity  $Z$ , an increase of  $Y$  translates into an increase of  $T_{eff}$  of the isochrone. This can be easily explained in term of quasi-homology relations and our grid of isochrones clearly confirms this behaviour (Figure 2).

Since for our 86 K dwarfs  $M_{Bol}$ ,  $T_{eff}$  and  $Z$  are known (Section 2) it is possible to infer the helium fraction  $Y$  with a simple interpolation over grids of the kind in Figure 2. Analogous grids exist between  $T_{eff}$  and mass (Figure 3) and  $Y$  and mass (Figure 4) so that from the isochrones it is also possible to infer the mass.

We use 5 Gyr old isochrones, half of the age of the disk (e.g. Jimenez et al. 1998) and consistent with the age of solar-type stars in its Neighbourhood (Henry et al. 1996), though the choice of the age is irrelevant since low mass stars are not evolved from the ZAMS. We have checked the use of 1 Gyr and 10 Gyr isochrones and the difference in the helium abundances are of order  $0.005 \pm 0.005$  and therefore

**Table 1.** Coefficients  $i = a, b$  for equation (1) and (2).

	$i_0$	$i_1$	$i_2$	$i_3$	$i_4$	$i_5$
$BC$	-7.67005	0.00248	-2E-7	9E-5	-0.44985	0.00672
$B - V$	4.96959	-0.00120	8E-8	-3E-5	0.29112	0.03581


**Figure 2.**  $\log(T_{\text{eff}})$ – $Y$  relation for different isochrones at three given values of  $M_{\text{Bol}}$ . Continuous lines connect squares of equal metallicity  $Z$ . The thick dash line refers to  $\Delta Y / \Delta Z = 6$ , the thin dash line to  $\Delta Y / \Delta Z = 0$ . Others dash lines refer to intermediate values. Notice that different  $\Delta Y / \Delta Z$  pivot around the temperature of our reference solar isochrone for the given  $M_{\text{Bol}}$ .

much smaller than those stemming from the uncertainties in  $T_{\text{eff}}$ ,  $M_{\text{Bol}}$ ,  $Z$ .

Some of the stars turn out to be outside the grid, meaning their inferred helium content lies outside the range covered by the isochrones. Since the grid is very regular and linear relations are also expected from quasi-homology, we have used a linear fit to extrapolate the helium content and the mass. As a consistency check we have also adopted another approach by fitting a second order polynomial between the helium content  $Y$  and  $T_{\text{eff}}$ ,  $M_{\text{Bol}}$  and  $Z$ . The helium abundances obtained with the two methods are identical to better than 0.01 meaning that the adopted extrapolation procedure has a negligible effect on the overall results. As a further test we have also used the MacDonald isochrones and the deduced helium abundances are always in very good agreement with those obtained with Padova ones, again confirming that our results do not depend significantly on the particular set of isochrones used.

## 4.2 Results

The behaviour of  $Y$  with  $Z$  is shown in Figure 5. Error bars for the helium abundances have been obtained via Monte-Carlo simulations, assigning each time values in parallaxes, metallicities, temperatures and bolometric luminosities with a normal distribution centered on the observed values and a standard deviation equal to the errors of the aforementioned quantities.

It is clear from Figure 5 that the helium-to-metal enrichment ratio is roughly linear for metallicities around and

above the solar one. A linear fit in this range is in fact able to recover within the errors the solar calibration value although the formal extrapolated primordial  $Y_P$  is underestimated with respect to Big Bang Nucleosynthetic estimates (Table 2).

A puzzling turnover in the helium content appears going to lower metallicities, with a break around  $Z = 0.013$ , reflecting what was qualitatively expected given the premises discussed in Section 3.3. Also, at lower metallicities the scatter in the data is larger. Such low helium abundances are clearly at odds with the latest primordial helium measurements from H II regions that range from  $Y_P = 0.2472$  to  $Y_P = 0.2516$  (Peimbert, Luridiana & Peimbert, 2007; Izotov, Thuan & Stasinska, 2007), even considering possible uncertainties in the zero-point of the solar  $Y_{\odot}$  value, which is a calibration parameter in stellar tracks (Section 3.2). Within present day accuracy, CMB data alone constrain the primordial helium mass fraction only weakly  $0.160 < Y_P < 0.501$  (Trotta & Hansen, 2004). What it is actually measured in CMB data is the baryon-to-photon ratio; once Standard Big Bang Nucleosynthesis is assumed a formally precise  $Y_P = 0.24815$  can be calculated (Spergel et al. 2006).

For metal poor stars a helium abundance close to the primordial value is what would be expected, with significantly lower values very difficult to explain. The need for sub-primordial helium abundances to fit the lowest metallicity stars in the Solar Neighbourhood with extant stellar models was already highlighted by Lebreton et al. (1999). Such a large discrepancy is evidently a challenge for stellar modeling and/or basic stellar data. In the next section we

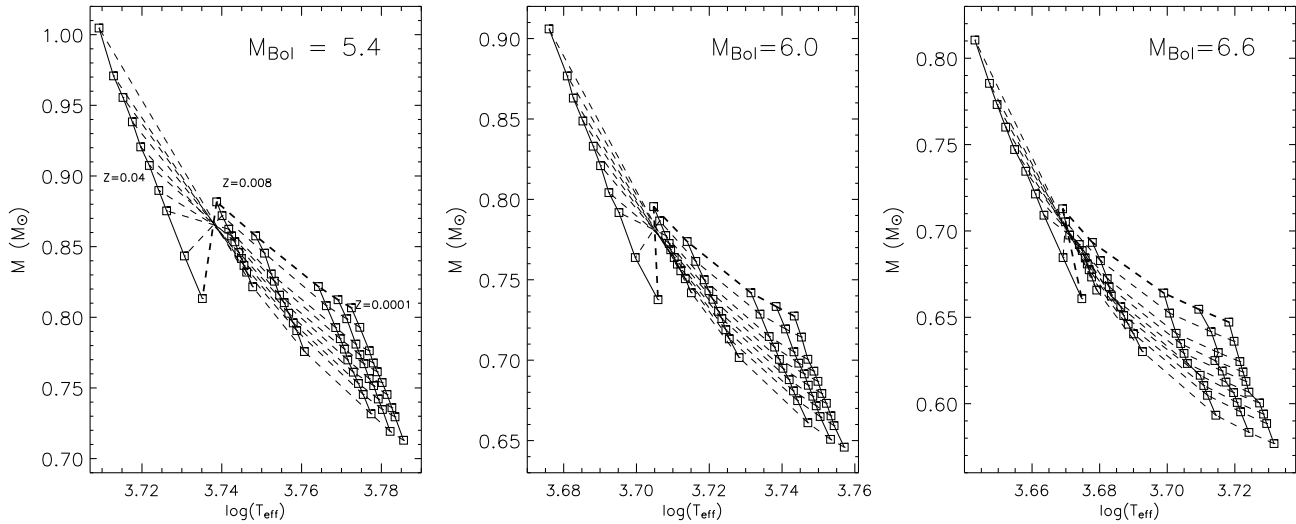


**Figure 3.**  $\log(T_{eff})$ –Mass relation for different isochrones at three given values of  $M_{Bol}$ . Same prescriptions as in the previous figure.

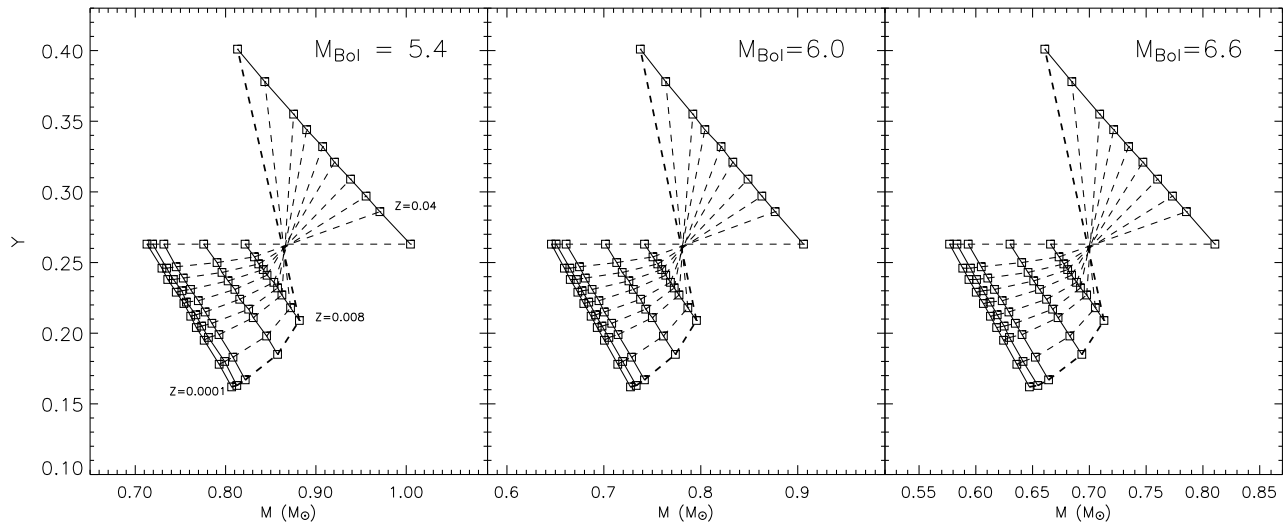


**Figure 4.** Mass–Y relation for different isochrones at three given values of  $M_{Bol}$ . Same prescriptions as in Figure 2.

**Table 2.** Linear fit with errors on both axis for the data in Figure 5.  $Y_{\odot}$  is the solar value recovered from the fit, to be compared with the value of 0.263 used to calibrate our solar model.

	$\frac{\Delta Y}{\Delta Z}$	$Y_P$	$Y_{\odot}$
$Z \geq 0.013$	$3.2 \pm 1.0$	$0.19 \pm 0.02$	$0.24 \pm 0.03$
$Z \geq 0.017$	$2.2 \pm 1.1$	$0.21 \pm 0.03$	$0.25 \pm 0.03$

carefully discuss to which extent such a large discrepancy can be reduced.

It is however clear that Figure 5 casts some doubts whether the hypothesis of a linear trend with constant  $\Delta Y/\Delta Z$  ratio is necessarily true over the entire  $Z$  range. Helium–to–metal enrichment factor determinations in literature have often made such an assumption for the sake of simplicity: in our case the ratio changes from 5 when all

stars are considered to 2 when only metallicity above the solar one are used : this may partly explain the very different measured values of  $\Delta Y/\Delta Z$  often reported in literature.

## 5 SEARCHING FOR PARTNERS IN CRIME

We discuss next various theoretical and observational uncertainties that could affect our results.

First we address whether the helium abundances correlate with parameters other than the metallicity then we focus on some open problems related to stellar models and finally to the adequacy of the adopted metallicity, temperature and luminosity scales.

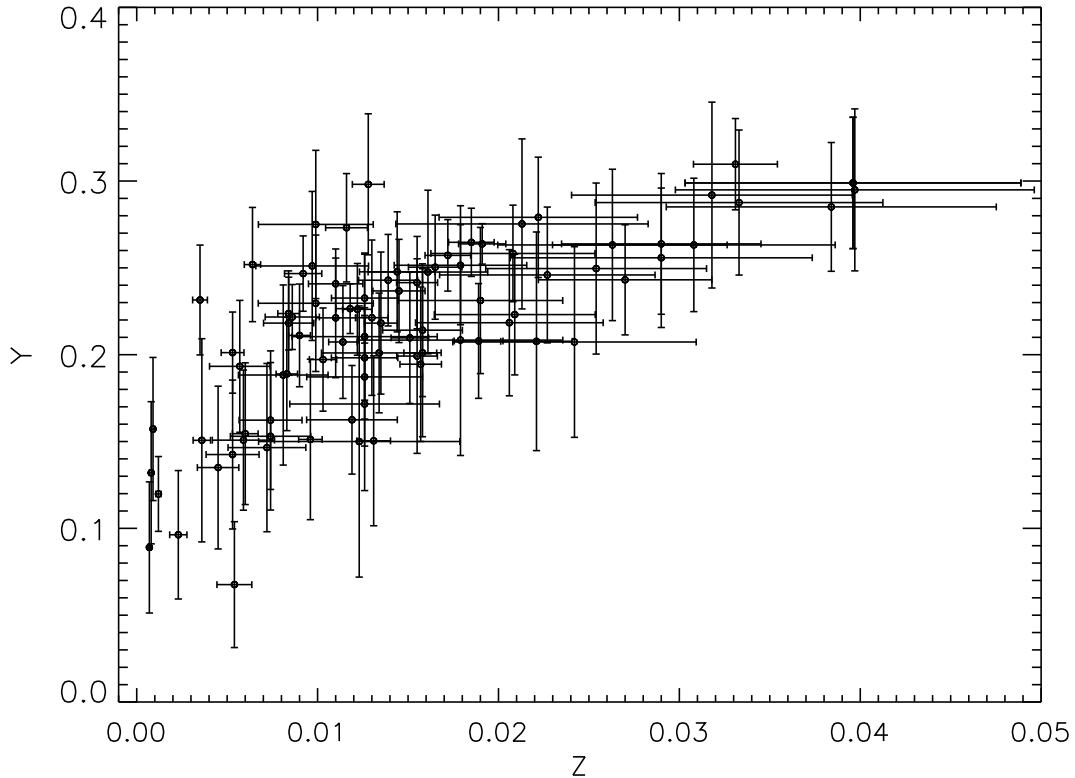


**Figure 5.** Helium ( $Y$ ) to metal ( $Z$ ) enrichment factor for our sample of stars. Error bars from MonteCarlo simulation according to the prescription given in the text.

### 5.1 Evolutionary effects

We have searched for any correlation between helium content and various parameters other than metallicity to highlight possible spurious trends in the models. Evolutionary effects are particular important, since low helium abundances could result from the attempt of fitting isochrones to stars that have already departed from their ZAMS and are thus brighter: in this case we expect a correlation between  $Y$  and  $M_{Bol}$ . Figure 6 shows the helium content as function of  $M_{Bol}$ ,  $T_{eff}$  and Mass (deduced from the isochrones). Since these plots have already built-in the  $Y - Z$  correlation that could mask or counterbalance other correlations, we have divided the sample into four metallicity bins to disentangle the underlying  $Y(Z)$  correlation from the others. No significant other correlation appears, besides the expected split between metallicity bins. At low metalicities, helium abundances below  $Y = 0.20$  are practically present for any value of  $M_{Bol}$ ,  $T_{eff}$  and mass.

The absence of any obvious trend is a posteriori confirmation of the adequacy of the adopted evolutionary cut  $M_{Bol} \geq 5.4$ . Figure 6 shows that most of our stars have masses (deduced from the isochrones) below  $0.85M_{\odot}$  at low  $Z$ . Studies of the oldest globular clusters in the Milky Way also confirm that metal-poor stars below  $0.80 - 0.85M_{\odot}$  have not yet reached the turn-off, the exact value depending on the age and the underlying details of the isochrones used to fit a globular cluster (e.g. Chaboyer et al. 2001, Morel & Baglin 1999). For higher metallicity the turn-off mass is also higher.

### 5.2 Shortcomings in stellar models

Despite the steady improvement in modeling stellar structure and evolution, there are still shortcomings in the theory that require the introduction of adjustable parameters, typically calibrated on the Sun.

Our model is accurately calibrated on the Sun, for an assumed  $Z_{\odot} = 0.017$ , by adjusting the helium content and the mixing-length in order to match its present age, radius and luminosity (Section 3.2). The  $Y_{\odot}$  value must be intended as the zero-point of our calibrated model and not as the absolute value of the solar helium content. Helioseismology does in fact return a lower helium content but including diffusion in the model helps to reduce such a difference (see Section 5.2.2). The difference between the present helium value derived from seismology and the initial value obtained from the calibration provides a constraint on the input physics of the model.

The fact that we are working with stars that are only slightly cooler and fainter than the Sun should ensure that we are studying a region of the HR diagram where models, at least for metalicities around the solar one, are well calibrated. Our solar isochrone is in fact in outstanding agreement with a sample of solar metallicity stars (Figure 7).

#### 5.2.1 Mixing-length

The universality of the mixing-length value is an open question. The analysis of binaries in the Hyades has recently lead

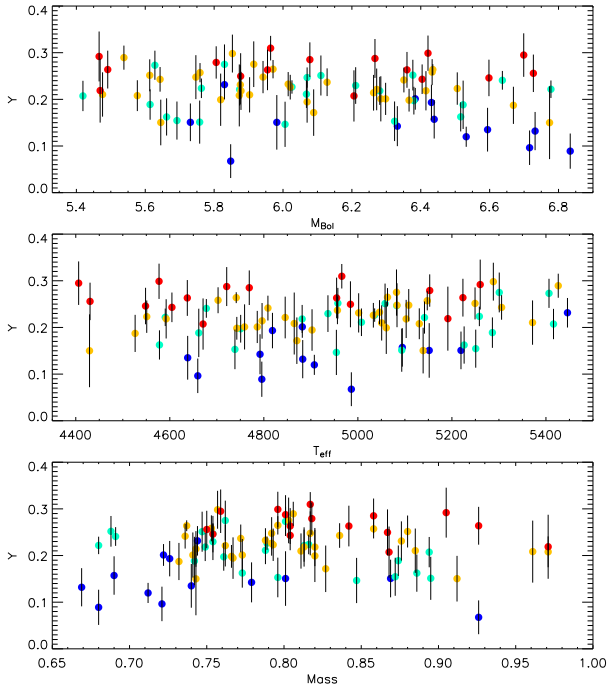


**Figure 6.** Helium content deduced from the isochrones as function of  $M_{Bol}$ ,  $T_{eff}$  and Mass for our 86 K dwarfs. Stars are divided in the same metallicity bins and colours as in Figure 1. No obvious dependence appears and low  $Y$  values are practically present throughout the entire range of parameters covered by our stars.

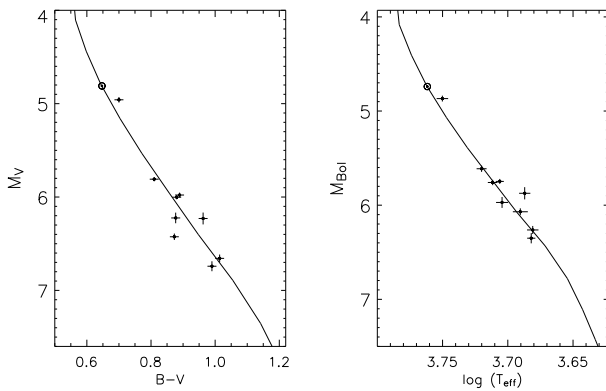


**Figure 7.** Comparison between 4.57 Gyr solar isochrone (age as determined from meteoritic measurements, Bahcall, Pinsonneault & Wasserburg 1995) and our sample stars in the  $[M/H]$  range  $\pm 0.04$  dex around the solar value. In order to have conservatively small errors we have used only stars with parallaxes better than 3%. Transformations to plot the solar isochrone in the observational plane as discussed in Section 3.3. Overplotted is also the Sun ( $\odot$ ) for which we have adopted colours and temperatures from Casagrande et al. (2006). The difference with the empirical  $B - V$  of Holmberg et al. (2006) is unnoticeable. Interestingly in the theoretical plane there is a much tighter agreement between model and observations.

Lebreton et al. (2001) and Yildiz et al. (2006) to conclude that the mixing-length increases with stellar mass. Similar conclusions were also drawn by Morel et al. (2000a) and Lastennet et al. (2003) based on the study of the binary systems  $\iota$  Peg and UV Piscium, respectively. These results are opposite to the theoretical expectation from hydrodynamical simulations of convection (Ludwig, Freytag & Steffen 1999; Trampedach et al. 1999). Detailed calibration of stellar models on the  $\alpha$  Cen system have returned discordant conclusions about the universality of the mixing length parameter (e.g. Noels et al. 1991; Edmonds et al. 1992; Neuforge 1993; Fernandes & Neuforge 1995; Morel et al. 2000b; Guenther & Demarque 2000). The latest model calibrations on the  $\alpha$  Cen system making use of seismic constraints favor a mixing-length that increases going to lower mass (Eggenberger et al. 2004, Miglio & Montalbán 2005) and therefore in agreement with the theoretical expectations. The discordant conclusions drawn from all these studies probably reflect the many observational uncertainties (order of magnitudes larger than for the Sun) in the input parameters of the models. These results suggest that at this stage a clear relation between mass and mixing-length is premature, either because uncertainties in the input parameters can overshadow shortcomings in the mixing-length theory itself, or because a dispersion of mixing-length at a given mass or even a time dependence of the mixing-length (Yildiz 2007) could well be possible. Therefore, assuming the solar mixing length is currently the safest choice. Systematic trends in mixing length are anyways overwhelmed by observational uncertainties.

As regards the dependence on the metallicity, the fact that all globular clusters require the same value for the mixing length parameter supports the assumption that it does not depend on  $Z$ , although such a conclusion is obtained studying giant branch stars (e.g. Jimenez et al. 1996; Palmieri et al. 2002; Ferraro et al. 2006). Concerning the particular region of the HR diagram we are going to investigate, models computed with the solar mixing-length reproduce the slope of the Main Sequence of young open clusters quite well (VandenBerg & Bridges 1984; Perryman et al. 1998) and of field stars (Lebreton et al. 1999) observed by *Hipparcos*. In addition, the study of Lower Main Sequence visual binary systems with known masses and metallicity returns a mixing-length unique and equal to the solar one for a wide range of ages and metallicities  $[Fe/H]_{\odot} \pm 0.3$  dex (Fernandes et al. 1998).

Nonetheless, a decrease of the mixing length at low  $Z$  would be particularly interesting since it would produce a less massive convection zone for a given stellar mass, thus making isochrones cooler. For metal poor stars this effect could partly alleviate the low helium problem. We have tested the effect of setting the mixing length  $\alpha_{MLT} = 1.00$  and the difference with respect to the adopted solar one ( $\alpha_{MLT} = 1.68$ ) is shown in Figure 8 for a moderately helium deficient and metal poor isochrone. As a result, a large change in the mixing length is indeed able to shift the isochrone to cooler temperatures, thus improving the agreement with the overplotted empirical isochrone. At the lowest masses covered by our study the disagreement is however still present, although reduced.

This result can be regarded as an indication of a metallicity dependence of the mixing-length for the Lower

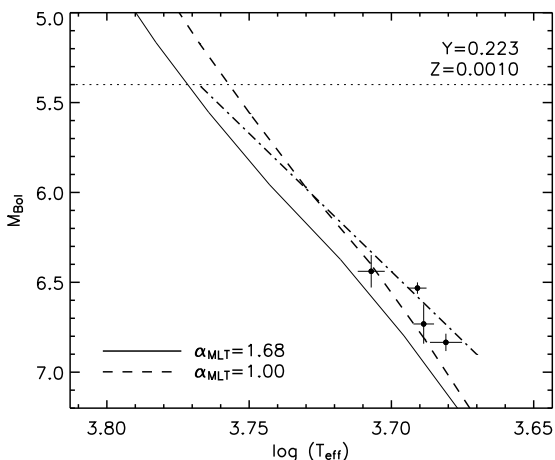


**Figure 8.** Effect of changing the mixing length  $\alpha_{MLT}$  in a metal poor isochrone (age 5 Gyr, although the age does not play any role). The dotted horizontal line in the left panel is the adopted cut in  $M_{Bol}$  for our sample of stars (see Section 2). Overplotted (dot dashed) is also our empirical isochrone for the same metallicity and our dwarfs with  $0.0007 \leq Z \leq 0.0013$ .

Main Sequence, as already suggested by Chieffi, Straniero & Salaris (1995). Whether such large change in  $\alpha_{MLT}$  is justified on other evidence or physical grounds remains to be seen. In this work we rather test to which extent the most recent low mass stellar models can be used *ipse facto* to study a large stellar sample in the Solar Neighbourhood. The range in which models can be safely used is discussed in Section 6.

### 5.2.2 Diffusion

Atomic diffusion (sometimes called microscopic or elemental diffusion) is a basic transport mechanism usually neglected in standard stellar models. It is driven by pressure, temperature and composition gradients. Gravity and temperature gradients tend to concentrate the heavier elements toward the center of the star, while concentration gradients oppose to the above processes (e.g. Salaris, Groenewegen & Weiss 2000). To be efficient, the medium has to be quiet enough, so that large scale motion cannot prevent the settling (e.g. Morel & Baglin 1999; Chaboyer et al. 2001). Diffusion acts very slowly, with time scales of the order of  $10^9$  years so that the only evolutionary phase where diffusion is efficient is during the Main Sequence<sup>3</sup>, in particular for metal poor (Population II) stars because of their small convective envelopes. For the Sun, the insertion of helium and heavy elements diffusion in the models has significantly improved the agreement between theory and observations (e.g. Christensen-Dalsgaard, Proffitt & Thompson 1993; Guenther & Demarque 1997; Bahcall et al. 1997; Basu, Pinsonneault & Bahcall 2000). Only in the region immediately below the convective envelope theoretical models deviate significantly from the seismic Sun, indicating that diffusion might not operate

<sup>3</sup> Diffusion turns out to be important also in White Dwarf cooling, but this is clearly outside the scope of this paper.

exactly in the way calculated or pointing to some neglected additional physical process partially counteracting diffusion (Brun et al. 1999).

Due to diffusion the stellar surface metallicity and helium content progressively decrease during the Main Sequence phase as these elements sink below the boundary of the convective envelope. In the deep interior, the sinking of helium towards the core leads to a faster nuclear aging, thus reducing the Main Sequence lifetime with consequences on the ages of Globular Clusters (Chaboyer et al. 1992; Castellani et al. 1997). In the envelope, diffusion leads to a depletion of the heavy elements and helium thus producing a decrease of the mean molecular weight. Metal diffusion decreases the opacity in the envelope and increase the central CNO abundance: the dominant effects are the decrease of the mean molecular weights in the envelope and its increase in the core which increases the model radius and hence decreases the effective temperature. The net effect on the evolutionary tracks, for a given initial chemical composition, is to have a Main Sequence cooler. Such effect reaches its maximum at the turn-off after which large part of the metals and helium diffused toward the center are dredged back in the convective envelope of giant branch stars, thus restoring the surface  $Z$  and  $Y$  to a value almost as high as for evolution without diffusion (e.g. Salaris et al. 2000).

Diffusion is clearly a major candidate in helping to solve the puzzling low helium abundances of Section 4, since it yields a cooler Main Sequence. Besides the effect on the stellar models themselves, diffusion affects the measured surface metallicities with respect to the true original ones of the stars, altering conclusions on  $Y(Z)$  (see below). In their pioneering work, Lebreton et al. (1999) found that Main Sequence models (for standard values of helium enhancement) were hotter than *Hipparcos* subdwarfs in the metallicity range  $-1 \leq [Fe/H] \leq -0.3$ . Since decreasing the helium abundance to resolve the conflict would have required values well below the primordial one (in accordance to what we have obtained in Section 3.3 and 4), Lebreton et al. (1999) advocated two processes that could help in solving the discrepancy : *i*) diffusion of helium and heavier elements in stellar models and *ii*) increase of the measured metallicity in metal poor objects due to usually neglected NLTE effects. Correcting isochrones for both effects they were partly able to solve the discrepancy (see also Morel & Baglin 1999), but their number of metal poor and faint stars was rather modest. Here we test the same corrections on many more stars.

We focus only on the effects of diffusion, leaving the discussion of observational uncertainties (among which NLTE effects) to Section 5.3. The works of Morel & Baglin (1999) and Salaris et al. (2000) specifically tackle the effects of helium and heavy elements diffusion in field stars. Both works assume a full efficiency of the diffusion so that their results can be regarded as an upper limit on its effects.

From the observational point of view, diffusion decreases the surface metallicity — provided that it is fully efficient and no other processes counteract it — so that a star presently observed with a given  $[Fe/H]$  has started its evolution with a larger metallicity  $[Fe/H]_0$ . As we discuss later such a difference is of order 0.1 dex, although sometimes higher differences have been claimed. Such a shift in metallicity has negligible effects on the fundamental param-

eters of  $T_{eff}$  and  $M_{Bol}$  determined for our stars with the IRFM (figure 11 in Casagrande et al. 2006), yet it would imply that our fits in Figures 2–4 are performed with too low  $Z$  isochrones, thus needing low  $Y$  values to compensate for the hot isochrone temperatures.

A proper comparison between diffusive and non-diffusive isochrones therefore must take into account also that diffusive isochrones must start their evolution with a higher metallicity so that at a chosen age their surface metallicity (which decreases with time) matches that of non-diffusive isochrones. Following the notation of Morel & Baglin (1999) we call isochrones that account for both effects (diffusion and correction of the surface metallicities) diffusive calibrated isochrones. Diffusion clearly introduces an age dependence regardless of the fact that stars are still on their ZAMS. As a general rule, depletion increases with increasing age since diffusion has more time to work. Differences between non-diffusive and diffusive calibrated isochrones are given by Salaris et al. (2000) for various metallicities, ages and luminosities. The calibrated diffusive isochrones are cooler by few tens up to 100–150 K, depending on mass and age (see figure 2 in Salaris et al. 2000). However, for the Lower Main Sequence the effect of diffusion becomes increasingly less significant (their table 1). At the lowest masses and faintest luminosities covered in this study the effect of diffusion is at most 30–40 K in  $T_{eff}$ . The reason for such negligible changes is that in the low mass regime, stars have large convective zones which inhibit diffusion. Figure 6 clearly shows that low values of helium are also found for objects with masses below  $0.7M_{\odot}$ , thus suggesting that diffusion is not the only possibility to solve the discrepancy. Similar results to those of Salaris et al. (2000) were also found by Morel & Baglin (1999) who give a large set of corrections between non-diffusive and diffusive calibrated isochrones. Their corrections are provided for 10 Gyr isochrones in the metallicity range  $0.0006 \leq Z \leq 0.006$  and masses between  $0.6$ – $0.85M_{\odot}$ . Their age is chosen in order to maximize the effect of diffusion. At this age, masses above  $0.85M_{\odot}$  start to evolve off the Main Sequence; for masses below  $0.6M_{\odot}$  the effect of diffusion is negligible. We apply these corrections to our isochrones and we consider only masses below  $0.85M_{\odot}$ . We linearly interpolate such corrections between contiguous values of  $M_{bol}$ ,  $T_{eff}$  and  $Z$  and apply them to all our sub-solar metallicities isochrones. In the range  $0.006 < Z < 0.017$  we have extrapolated them. Notice that the corrections in Morel & Baglin (1999) are given for isochrones with standard values of  $Y(Z)$  whereas here we apply them to isochrones with a large range of  $Y(Z)$ . However, the main effect of diffusion is to alter the surface  $Z$  and that does not depend on  $Y$ .

The results of computing the helium abundances for our stars with the corrected isochrones are shown in Figure 9. Diffusion clearly helps in increasing the inferred helium fractions and its effect—as expected—becomes more important going to lower metallicities. However extremely low helium abundances at the lowest  $Z$ 's are still found. The fact that low helium abundances are now preferentially found among the fainter and less massive stars reflects the fact that—as anticipated—corrections due to diffusion become less and less important descending along the Main Sequence. Still, disturbingly low values of  $Y \sim 0.2$  remain for any mass and

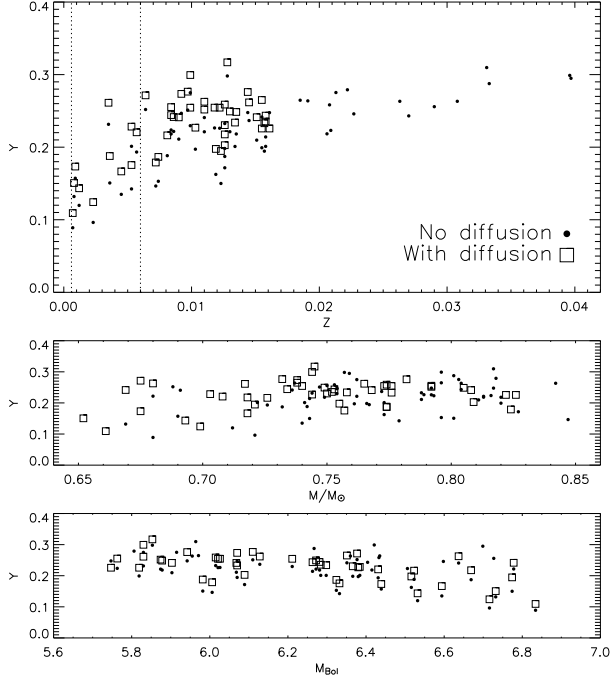


**Figure 9.** First panel:  $Y$  versus  $Z$  plot when the effects of diffusion are included (squares) or not (circles) in the computation. The vertical dotted lines are the metallicity range for which Morel & Baglin (1999) give corrections. We have extrapolated such corrections up to the solar metallicity  $Z = 0.017$ . For higher metallicities only circles are shown. Second and third panel: dependence of  $Y$  with Mass and  $M_{Bol}$ . Error bars are not shown for clarity purpose, but are of same magnitude as in Figure 5 and 6.

luminosity, although more orthodox values are within the error bars.

Until now we have estimated the effect of diffusion in the case of full efficiency of this process. However there are many observational evidences suggesting diffusion is less effective.

Diffusion is expected to be more important in metal poor stars, where the mass of the convective envelope is smaller (e.g. Chaboyer et al. 2001); however, whether it effectively occurs and how efficiently is still matter of debate, especially at low metallicities. Observations of the narrow Spite Li-plateau in metal-poor stars (Spite & Spite 1982; Thorburn 1994; Ryan, Norris & Beers 1999; Asplund et al. 2006; Bonifacio et al. 2007) suggest that diffusion is inhibited near the surface of these objects (e.g. Deliyannis & Demarque 1991; Chaboyer & Demarque 1994; Ryan et al. 1996) although Salaris & Weiss (2001) pointed out that after carefully accounting for uncertainties and biases in observations, models with diffusion are still in agreement with observations. More recently Richard et al. (2005) invoked a ‘turbulent diffusion’ which would limit diffusion without mixing Li. If Li does not allow firm conclusions,  $[Fe/H]$  is a much more robust diagnostic (e.g. Chaboyer et al. 2001). The absence of any variation in  $[Fe/H]$  between giant branch and turn-off stars found by Gratton et al. (2001) for two globular clusters (NGC6397 with  $[Fe/H] = -2.03$  and NGC6752 with  $[Fe/H] = -1.42$ ) is a very strong evidence that sedimentation cannot act freely in all stars. Regarding field stars, diffusion must affect the measured  $[Fe/H]$  only marginally oth-

erwise high-velocity giants in the *Hipparcos* catalogue would have on average metallicity that are larger by a factor of two than their turn-off or Main Sequence counterparts, a feature which has not been observed (D'Antona et al. 2005b).

Diffusion also changes the slope of the Main Sequence, rendering it steeper as one goes to higher luminosities (Morel & Baglin 1999; Salaris et al. 2000). Figure 2 suggests that our empirical isochrones roughly agree with theoretical ones and increasing the theoretical slope in the upper part of the Main Sequence would actually reduce the agreement. Also, the effect of diffusion produces a distortion in the mass-luminosity relation (Morel & Baglin 1999) so that extremely accurate data could, in principle, detect it. Interestingly, within the present day accuracy, our results agree with mass-luminosity relations (see Section 7). Since the efficiency of diffusion changes with metallicity—if diffusion actually occurs—a much larger sample of disk stars than those used in this study (so that the time on which diffusion has been acting is on average the same and equal to the mean age of the disk) would probably make possible to detect a change in the slope of empirical isochrones between metallicity say, solar and a third solar. We have tried to add a  $\log Z \times \log T_{\text{eff}}$  term in equation (3) to roughly account for a possible change in the slope, without finding any noticeable effect although in our case the noise could dominate over such a tiny signal.

Also from the point of view of theoretical modeling, the effect of heavy element diffusion in metal poor stars is still controversial (e.g. D'Antona et al. 2005b; Gratton, Sneden & Carretta 2004) as theoretical results also differ according to the formalism employed to describe it. Models that assume complete ionization (and then negligible effects of radiation pressure) predict depletion for all elements heavier than H (e.g. Straniero, Chieffi & Limongi 1997; Chaboyer et al. 2001). However, accounting for partial ionization and radiation pressure shows that whereas some elements like He and Li are expected to be depleted, others (like Fe) are expected to be significantly enhanced for stars with  $T_{\text{eff}} > 6000$  K and only moderately underabundant ( $\sim 0.1$  dex or less) below this temperature (Richard et al. 2002). Chaboyer et al. (2001) found that models with full diffusion differ by more than  $2\sigma$  from the observations of Gratton et al. (2001), thus concluding that heavy-element diffusion does not occur in the surface layers of metal-poor stars and that isochrones including the full effects of diffusion should not be used for comparison with observational data. Although it is not yet clear which mechanism can counteract diffusion in the surface layers—mass loss (Vauclair & Charbonnel 1995), mixing induced by rotation (e.g. Vauclair 1988; Pinsonneault et al. 1992, 1999, 2002) and radiative diffusion (Morel & Thévenin 2002) have been proposed among others—Chaboyer et al. (2001) found that the temperatures of models in which diffusion is (admittedly ad hoc) inhibited near the surface (but not in the deep interior) of metal poor stars are similar to the temperatures of models evolved without diffusion. Also Richard et al. (2002) concluded that at least in  $0.8M_{\odot}$  stars, it is a better approximation not to let Fe diffuse than to calculate its gravitational settling without including the effect of radiative acceleration.

In summary, all models predict the effect of diffusion to increase with decreasing metallicity, since at lower  $Z$  the Main Sequence shifts to hotter temperatures, for which con-

vective layers are smaller. At the same time, Lithium (to some extent) and the most accurate [Fe/H] measurements in globular clusters (Gratton et al. 2001) pose an upper limit to the effect of diffusion that even for the most metal poor stars in our sample is expected (if any) to be negligible or within our error bars. The results shown in Figure 9 assume a fully efficient diffusion that is improbable and still does not solve the low helium abundances.

### 5.3 NLTE effects and adopted temperature and luminosity scale

As previously mentioned, Lebreton et al. (1999) were partly able to resolve the low helium abundance problem by using the cumulated effect of diffusion and NLTE departures in metallicity measurements. According to Thévenin & Idiart (1999) NLTE corrections are negligible for stars with solar metallicity but for  $[\text{Fe}/\text{H}] \sim -1.0$  the measured metallicity should be increased of order 0.15 dex (the larger corrections being for hotter  $T_{\text{eff}} > 6000$  K—stars that however we do not have in our sample). Such a difference, although significant is roughly of the same order of present day uncertainties in abundance determinations. Besides, the relatively large differences claimed by Thévenin & Idiart (1999) have not been confirmed by other subsequent works. Gratton et al. (1999) found negligible departures from LTE in dwarf stars of any  $T_{\text{eff}}$  concluding that LTE abundance analysis of metal poor dwarfs are validated, an important support to the current views on galactic chemical evolution. Gratton et al. (1999) also analyzed NLTE effects on species other than Fe and again they did not find any significant departures in the case of cool dwarfs. Similar conclusions were drawn by Fulbright (2000) and Allende Prieto et al. (1999) pointed out that NLTE starts to show up primarily at  $[\text{Fe}/\text{H}] < -1.0$  (i.e.  $Z \lesssim 0.003$  whereas our low Y values are already found at higher metallicities). Thorough calculations accounting for NLTE effects have been carried out by Gehren et al. 2001a, 2001b; Korn, Shi & Gehren 2003 who found negligible corrections for the Sun and up to 0.06 dex in the case of halo stars. The effects of departures from LTE in abundance determinations of various elements are widely discussed in Asplund (2005). Summarizing, in the case of Iron lines a clear consensus about NLTE effects is still far from reach, but it seems reasonable to assume that corrections of order 0.10 dex are expected in stars with low metallicities and/or  $\log g$ .

The metallicities we use come from various sources (Casagrande et al. 2006), so that this might account for part of the scatter in the data. However, the overall trend is clear and therefore does not depend on the specific metallicity scale adopted. Besides, in the colour-colour planes (especially in the  $B - V$  colour index which is very sensitive to metallicity) there is a very good agreement between our sample of stars and the homogeneous metallicity scale of model atmospheres (Casagrande et al. 2006). We have already mentioned that our work is differential with respect to the Sun and therefore we expect our results to be unaffected by the new solar abundances obtained when 3D modes atmospheres are adopted, provided that similar updates pertain also the lower Main Sequence stars. However, large libraries of 3D model atmosphere for analyzing stellar spectra are not yet

available. Therefore, we can not exclude *a priori* some sort of effect depending on  $Z$ .

We also test whether the low helium abundances depend on the adopted temperature and luminosity scale. Our empirical IRFM temperature (and luminosity) scale is in agreement with spectroscopic measurements and  $\sim 100$  K hotter than other IRFM temperature scale (see Casagrande et al. 2006 for a detailed discussion); it closely recovers the temperatures of a set of solar analogs and indeed the theoretical solar isochrone is in outstanding agreement with the data (Figure 7). Cooler temperature scales clearly tend to increase the disagreement with respect to theoretical isochrones, although when studying the HR diagram it is the combined effect of temperature *and* luminosity scales to be important. In this respect, the IRFM is one of the few methods that returns a fully consistent temperature and luminosity scale.

If we adopt the IRFM scale of Ramírez & Meléndez (2005) by decreasing our effective temperatures by 100 K and luminosities by 1.4% (Casagrande et al. 2006) the problem of low helium abundances gets even worse. The shape of the  $Y$  vs.  $Z$  plot is the same (reflecting the offset in the absolute calibration adopted, Casagrande et al. 2006) but the helium content is on average lower by  $\sim 0.04$  so that already at solar metallicity the bulk of stars has a helium content lower than our solar calibrated model.

## 6 THE BINARY TEST

To date, the most stringent tests of the theory of stellar structure and evolution have been carried out for the Sun. Its mass, luminosity and radius are known to better than 1 part in  $10^3$  and its age to better than few percent (e.g. Guenther & Demarque, 2000; Bahcall, Serenelli & Basu 2006). Its chemical abundance, which sets the zero point of metallicity measurements in other stars, is currently under profound discussion (Asplund et al. 2005) however, as we have already mentioned, this change should not affect dramatically our study since our work is differential with respect to the Sun. The Sun is therefore the natural benchmark in understanding and setting models of stellar structure and evolution. We have already checked the solar isochrone to be in excellent agreement with our solar metallicity stars (Figure 7).

In the case of stars other than the Sun, radii and luminosities are known with much less accuracy although interferometry is expected to be a major breakthrough in the next few years. Still, masses can be empirically determined only in the case of binaries. For visual binary systems with well-measured parallaxes, the uncertainty in mass determination is rarely less than 1%, a value that sets the accuracy required to provide important constraints on models of stellar structure and evolution (e.g. Andersen 1991). In addition to the mass, the measured colours and metallicities are another source of errors.

As we have already discussed in Section 4 such limitations preclude the accurate calibration of stellar models on binary stars. Our model is calibrated on the Sun but the comparison with a statistically congruous number of binaries can indeed provide important constraints on it. Here we use various double stars with accurately measured masses, metallicities and colour indices for at least one of the com-

ponents. They are all nearby, so that no reddening corrections are needed. Colours and metallicities are used to derive  $T_{eff}$  and  $M_{Bol}$  consistently with our IRFM scale. The mean metallicity from various recent measurements is used so as to reduce the uncertainty in this observable. The same procedure described in Section 4 is then applied to deduce the mass and the helium content of these binaries. To have a congruous number of stars, we have slightly relaxed our cut-off on  $M_{Bol}$ . All the binaries have relatively low masses so that the helium abundances are insensitive to the age of the isochrones that we set to 5 Gyr (see Section 4), if not otherwise specified. Although the broadening (and so the helium content) of the Lower Main Sequence is independent of the age, masses shift along the isochrones with age. Such a drift along the isochrones is rather small in the Lower Main Sequence, but makes masses not completely age independent. We have tested the difference in the resulting masses if 1 Gyr and 10 Gyr old isochrones are used, instead. With respect to the adopted choice of 5 Gyr, younger (older) isochrones yield masses larger (smaller) by at most  $\sim 0.03M_{\odot}$ . Such differences are of the same order of the errors given in Table 3, however 5 Gyr old isochrones are representative of the mean age of disk stars also considering that the age–metallicity relation has been proven to be rather weak (e.g. Feltzing et al. 2001) so that older isochrones are not necessarily the most appropriate for metal poor stars. We mention that all these stars belong to binary systems without interaction so they are representative of single stars.

The mass deduced from the isochrones is compared to the mass measured empirically: if the mass is recovered with an accuracy of few percent the corresponding helium content of the star is also validated (Figure 4).

### 6.1 $\alpha$ Cen B

Among stars other than the Sun, the  $\alpha$  Cen system is probably the most used test-bed for checking stellar models (see also discussion in Section 5.2.1). Its secondary component (HD 128621) is a K dwarf and it has been a privileged target for asteroseismic (e.g. Thévenin et al. 2002, Kjeldsen et al. 2005) and interferometric (Kervella et al. 2004, Bigot et al. 2006) studies. Since it is a well separated binary this star is part of our original sample of Section 2, but here we analyze the results with some more detail. Using positions and radial velocities its mass has been estimated to great accuracy ( $M = 0.934 \pm 0.0061 M_{\odot}$ ) and completely independently of theoretical considerations of stellar structure and evolution (Pourbaix et al. 2002). For this star there are various independent and accurate metallicity measurements (Valenti & Fischer 2005, Santos et al. 2005, Allende Prieto et al. 2004, Feltzing & Gonzalez 2001) with a mean value  $[Fe/H] = 0.23 \pm 0.03$  dex and solar scaled abundances. Accurate  $BV(RI)_C$  colours (Table 3) are available from Bessell (1990) from which  $T_{eff}$  and  $M_{Bol}$  are computed as described in Section 2. We obtain a mass of  $0.927 \pm 0.039 M_{\odot}$  in excellent agreement with that measured empirically. The corresponding helium content is found to be  $0.263 \pm 0.028$  and therefore equal to the solar one, although the star is more metal rich.

## 6.2 vB22

As summarized by Lebreton et al. (2001), the Hyades cluster has five binaries whose components have measured masses. Of these systems only HD 27130 (vB22) has masses with small enough uncertainty to place significant constraints on the theoretical models and to this purpose it has also been studied by Pinsonneault et al. (2003). For this eclipsing binary  $BV(RI)_C$  magnitudes and colours of both components are available from Schiller & Milone (1987) and are listed in Table 3. Again,  $T_{eff}$  and  $M_{Bol}$  are derived according to the procedure described in Section 2. Though metallicity measurements for an eclipsing binary are quite uncertain, we exploit the fact that the metallicity of such a system must be the same of other cluster's members. For the Hyades' members, Paulson, Sneden & Cochran (2003) have conducted a detailed spectroscopic analysis from which a mean metallicity  $[Fe/H] = +0.13 \pm 0.04$  dex and solar scaled abundances have been derived. High-precision distance estimates are available from *Hipparcos* ( $\omega = 21.40 \pm 1.24$ ) and from kinematic parallax (de Bruijne et al. 2001,  $\omega = 21.16 \pm 0.38$  mas). These are all in excellent agreement and we assume de Bruijne et al. (2001) measurement in the following.

Empirical masses are available from Torres & Ribas (2002). For the mass and bolometric magnitude of the primary, age effects become relevant and, rather than our standard reference 5 Gyr isochrones, we consider isochrones of 500 Myr (1 Gyr), consistent with the age of the cluster (Perryman et al. 1998). The estimated mass is  $1.104$  ( $1.091$ )  $M_{\odot}$  ( $1\sigma$  more massive than the empirical value) and the corresponding helium content  $Y \sim 0.22$ . Optimizing on the mass formally returns an age of 2.67 Gyr and  $Y \sim 0.23$ . Evidently age effects are important here, but in any case, the helium content of the system is significantly below solar. For the secondary, as expected, the mass and the helium content are independent of the age chosen for the isochrones. The difference in the use of 500 Myr and 5 Gyr isochrones is less than 0.01 in mass and 0.005 in helium abundance, i.e. smaller than the uncertainty of the results. Using 5 Gyr isochrones, the mass we recover for the secondary is in very good agreement with the empirical one, with a helium content significantly lower than the solar one. Though depending also on the exact metallicity of the binary (we have assumed the average value of the cluster, but a slight scatter among its stars is possible), our result provide a further, strong evidence that the Hyades are underabundant in helium for their metallicity (Perryman et al. 1998; Lebreton et al. 2001; Pinsonneault et al. 2003).

## 6.3 70 Oph

70 Oph (HD 165341) is one of our nearest neighbours and is among the first discovered binary stars. Gliese & Jahreiß (1991) classify it as a primary of spectral type K0 V and a secondary K5 V. Recent abundance analysis for the primary companion are available from Luck & Heiter (2006), Mishenina et al. (2004), Allende Prieto et al. (2004). We adopt the mean value  $[Fe/H] = -0.02 \pm 0.08$  dex and  $[\alpha/Fe] = 0.06 \pm 0.11$  dex. Tycho  $B_T$  and  $V_T$  magnitudes for both components are available from Fabricius & Makarov (2000) which we convert to the Johnson-Cousins system interpolating the transformation coefficient given in table 2

of Bessell (2000). Additional photometry is available from Gliese & Jahreiß :  $V$  magnitudes agree with the transformed Fabricius & Makarov (2000) ones within 0.01 mag, whereas the  $B - V$  index of Gliese are slightly ( $0.02 - 0.04$  mag) redder.  $(R - I)_K$  from Gliese & Jahreiß has been converted to the Cousins system with the transformation given in Bessell (1995). For consistency with the choice done for most of the binaries we use only magnitudes and colours from Gliese & Jahreiß. Averaging with the  $B$  and  $V$  magnitudes from Fabricius & Makarov (2000) hardly changes the results : the large uncertainty in  $T_{eff}$  for the primary component remains the same and the changes in the helium content and masses of both components are smaller than their final errors. We use the *Hipparcos* parallax and errors as corrected by Söderhjelm (1999) ( $\omega = 195.70 \pm 0.90$  mas) for binarity effects. Masses for the primary and the secondary are available from Henry & McCarthy (1993) ( $M = 0.856 \pm 0.056 M_{\odot}$  and  $M = 0.713 \pm 0.029 M_{\odot}$ , the secondary as recomputed with improved parallax by Delfosse et al. 2000) and from Fernandes et al. (1998) ( $M = 0.89 \pm 0.04 M_{\odot}$  and  $M = 0.71 \pm 0.04 M_{\odot}$ ) that we assume in the following<sup>4</sup>. Based on asteroseismic considerations Carrier & Eggenberger (2006) also derived a mass of  $0.87 M_{\odot}$  for the primary component. The masses we derive are in good agreement with the empirical ones although the large uncertainty in  $T_{eff}$  of the primary returns considerably large error bars. The helium content is equal to the solar one within the errors, consistently with the expectation given the solar metallicity. A solar helium abundance was also obtained by Fernandes et al. (1998).

## 6.4 $\xi$ Boo

$\xi$  Boo (HD 131156) consists of a primary of spectral type G8 V and a secondary K4 V (Gliese & Jahreiß 1991). The primary is known to be very active with irregular fluctuations of activity (e.g. Petit et al. 2005 and references therein) and a high chromospheric emission (Baliunas et al. 1995) being classified as flare star in SIMBAD and variable in *Hipparcos*. These data suggest a young age that also agrees with conclusions from evolutionary models (Fernandes et al. 1998). Recent abundance analyses for the primary component are available from Luck & Heiter (2006), Valenti & Fischer (2005), Allende Prieto et al. (2004), Fuhrmann (2004). We adopt the resulting mean value  $[Fe/H] = -0.15 \pm 0.09$  dex and  $[\alpha/Fe] = -0.06 \pm 0.15$  dex.  $V$  magnitudes,  $B - V$  and  $(R - I)_K$  indices of both components are available from Gliese & Jahreiß (1991). We convert  $(R - I)_K$  into Cousins system by means of the Bessell (1995) transformations. Improved *Hipparcos* parallaxes are available from Söderhjelm (1999) and empirical masses from Fernandes et al. (1998).

Our results are interesting : the primary is almost  $1\sigma$

<sup>4</sup> Note that Fernandes et al. (1998) calibrated stellar models on some of the binaries we also discuss in this Section. Their approach is quite different from ours since they had helium content, age, mixing-length and individual masses of both components as free parameters in the model. However, they also computed empirical masses of both components and used the sum as a constraint on the model. In the following Section we only use their empirical masses for comparing our results.

more massive than the empirical value, whereas the secondary is  $2\sigma$  less massive. Also, the helium content between the two component differs by more than  $1\sigma$ , whereas all the other binaries in this study have identical helium abundances within the errors. To reach a closer agreement with the empirical masses, that of the primary should be decreased (implying a higher helium abundance, see Figure 4) whereas that of the secondary should be increased (thus lowering its helium content). The photometry for these two objects can be easily influenced by the young age induced variability thus explaining these puzzling results. Torres et al. (2006) found chromospheric activity as a likely cause of the discrepancy between models and observations in the case of another star (HD 235444). Therefore we discard this binary in the following discussion.

One might wonder whether variability can occur among some of the stars in Section 2 and to which extent this can explain anomalous helium abundances. Extensive surveys by *Einstein* and *ROSAT* and *Chandra* X-ray satellites have shown that late-type Main Sequence stars are surrounded by coronae analogous to the more easily observed solar corona (e.g. Schmitt & Liefke 2004, Wood & Linsky 2006). Flares, spots, coronal mass ejections, prominences are, of course, not exclusive to our Sun. For our sample of stars we have used the  $\Delta\mu$  method to remove unsolved binaries (whose tidal interaction could trigger activity, e.g. Torres et al. 2006) and the same sample is also free from variable stars to a high accuracy level (Casagrande et al. 2006). Therefore, any intrinsic level of activity in the sample of Section 2 is below our observational uncertainties and does not bear on the comparisons with theoretical isochrones. Furthermore, to explain the low helium abundances variability should practically and exclusively occur in metal poor stars, a correlation that appears to be very unlikely.

## 6.5 HD 195987

Combining spectroscopic and interferometric observations, for this double-lined binary system, Torres et al. (2002) derived masses with a relative accuracy of few percent. They also determined the metallicity ( $[\text{Fe}/\text{H}] = -0.5$ ,  $[\alpha/\text{Fe}] = +0.4$  and uncertainty  $\sim 0.2$  dex), orbital parallax ( $\omega = 46.08 \pm 0.27$  mas in rough agreement with the *Hipparcos* value, but with smaller formal error) and  $V, H, K$  magnitudes for both components. Their infrared magnitudes are in the CIT system and we convert them into the 2MASS by using the Carpenter (2001) transformations. We then use our effective temperature and bolometric luminosity calibrations and the procedure described in Section 4 to deduce the mass and helium content of both components. The mass of the primary is higher by  $3\sigma$  but that of the secondary only by  $1\sigma$ . Both components are fitted with practically identical helium content. Ascribing the mass discrepancies to temperature effects, an increase of 100 K in the  $T_{\text{eff}}$  of the secondary (or more properly a corresponding decrease in the effective temperature of the isochrones) would return a mass ( $0.662M_{\odot}$ ) in excellent agreement with the empirical one, but the helium content would be still very low ( $Y = 0.182$ ). For the primary the temperature should be increased by 300 K in order to obtain a mass ( $0.842M_{\odot}$ ) in agreement with the empirical one. In this case the helium content would be  $Y = 0.269$ , higher than that of our solar calibrated model. However, the

primary is very luminous given its mass, so that it could be a slightly evolved stars and therefore 5 Gyr isochrones could not be the most appropriate choice. If 10 Gyr isochrones are used, masses are decreased so that the primary is off by  $2\sigma$  and both components are again fitted with the same helium content.

## 6.6 $\eta$ Cas B

$\eta$  Cas (HD 4614) is a nearby visual binary at a distance  $\sim 6$  pc. According to Gliese & Jahreiß (1991) it consists of a primary of spectral type G3 V and a secondary K7 V.  $\eta$  Cas A is known to be over-luminous with respect to the mass-luminosity relation, thus suggesting that it has begun to evolve off the Main Sequence (Fernandes et al. 1998). In what follows we focus on the secondary,  $\eta$  Cas B. Abundance analysis for cool dwarfs are still challenging (e.g. Bonfils et al. 2005), however the metallicity of the primary is well determined. We have taken five independent metallicity measurements (most of which include  $\alpha$ -elements) from Luck & Heiter (2006), Valenti & Fischer (2005), Bonfils et al. (2005), Mishenina et al. (2004), Allende Prieto et al. (2004). All these measurements show good agreement and we adopt a mean value of  $[\text{Fe}/\text{H}] = -0.31 \pm 0.07$  dex and  $[\alpha/\text{Fe}] = 0.10 \pm 0.03$  dex. Visual magnitude,  $(B - V)$  and  $(R - I)_K$  colours for the secondary are also available from Gliese & Jahreiß (1991).  $(R - I)_K$  is in the Kron system and it has been converted to the Cousins system with the transformation given in Bessell (1995). Both colours are slightly redder than the applicability range of our temperature and bolometric luminosity calibrations, consistently with the late spectral type of this star. However the mean loci of the calibrations in Casagrande et al. (2006) (see their figure 13 and 18) show well defined trends so that the extrapolation to stars  $\sim 100$  K cooler than the applicability range is still quite reasonable. The parallax of the primary is available from *Hipparcos* and the mass of the secondary from Fernandes et al. (1998). Notice that both the spectral type and the mass of this star are slightly lower than that of our sample stars in Section 2, however it is still interesting to check how isochrones behave at this lower limit. The result for this moderately metal deficient star is particularly interesting, since it has a low helium abundance (but in agreement with the bulk of stars with same metallicity in Figure 5) and its mass is lower than the empirical value. At this metallicity NLTE effects in the derived metallicities should be very small if any, as well as the effect of diffusion that are negligible at  $0.6M_{\odot}$ . Also, from Figure 4 an increase of the mass at fixed metallicity would require an even lower helium abundance.

As we have already mentioned Fernandes et al. (1998) calibrated stellar models to this binary obtaining a helium content ( $Y = 0.25$ ) higher than that found here. However, considering the difference in the respective solar reference value (their solar model has  $Y_{\odot} = 0.28$ ) our result is within  $1\sigma$  with theirs.

## 6.7 85 Peg A

85 Peg (HD 224930) is a well studied, metal poor, visual and single-lined spectroscopic binary. Its small angular separation and the marked magnitude difference between the

components ( $\Delta m_V = 3.08 \pm 0.29$  mag, ten Brummelaar et al. 2000), makes it a difficult target both for visual and spectroscopic observations. The given  $\Delta m_V$  implies a magnitude correction of 0.06 mag for the primary that increases going to longer wavelength (0.12 mag in  $I$ , see equation 4). The contribution of the secondary thus must be properly removed. The total mass of the system is well constrained from visual orbital elements and Kepler's Third law (e.g. Griffin 2004; Fernandes et al. 2002) however the masses of the individual components are much more uncertain.

For the primary 85 Peg A, we adopt a mass of  $0.84 \pm 0.08 M_\odot$ , obtained by Fernandes et al. (2002) and in qualitative agreement with D'Antona et al. (2005b) who, based on model predictions, estimated the mass to be in the range 0.75 to  $0.82 M_\odot$ . For many years investigators have claimed that 85 Peg B, the fainter companion, is more massive than 85 Peg A, the brighter one (e.g. Hall 1948; Underhill 1963; Heintz 1993) and this abnormal situation could be explained if 85 Peg B is an undetected binary, as already suggested by Hall (1948). Indeed, this seems to be the case, as the same conclusions can be drawn when the position of both components in the HR diagram is compared with theoretical expectations (Fernandes et al. 2002; D'Antona et al. 2005b). In what follows we only consider the primary component. We use the *Hipparcos* parallax and errors as corrected by Söderhjelm (1999) ( $\omega = 82.50 \pm 0.80$  mas) for binarity effects. For the metallicity we adopt the mean value obtained from six recent independent determinations (Luck & Heiter 2006; Mishenina et al. 2004; Allende Prieto et al. 2004; Fuhrmann 2004; Gratton et al. 2003; Fulbright 2000). All these measurements show good agreement with an average  $[\text{Fe}/\text{H}] = -0.90 \pm 0.06$  dex and  $[\alpha/\text{Fe}] = +0.40 \pm 0.04$  dex. Spectroscopic determinations return temperatures ranging from  $\sim 5300$  K (Fulbright, 2000) to  $\sim 5600$  K (Fuhrmann, 2004), the latter being in close agreement with other recent determinations obtained carefully fitting Balmer line wings (D'Antona et al. 2005b). A temperature of about 5600 K seems to be favored also by stellar modeling (Fernandes et al. 2002; D'Antona et al. 2005b). By means of adaptive optics, ten Brummelaar et al. (2000) obtained  $VRI$  differential photometry of the components, from which individual magnitudes were then deduced using the mean composite magnitudes found in the General Catalogue of Photometric Data (Mermilliod, Mermilliod & Hauck 1997). With the individual magnitudes given by ten Brummelaar et al. (2000) we obtain  $T_{\text{eff}} = 5000 \pm 350$  K,  $M_{\text{Bol}} = 5.06 \pm 0.07$  mag and an angular diameter that, translated into linear radius via parallax, is equal to  $1.15 \pm 0.15 R_\odot$ . Besides a temperature much smaller than other determinations, the returned linear radius seems to be excessively large for a star with a mass well below that of the Sun. Furthermore, in the catalogue of Absolute Radii of Stars compiled by Pasinetti-Fracassini et al. (2001) the mean linear radius obtained with various indirect techniques is  $0.84 R_\odot$ . Prompted by such a puzzling result, we have made an independent search for accurate photometry, rather than using a generic mean value. In particular, we caution that Johnson  $RI$  bands lack a clearly defined set of standard (e.g. Bessell 1979, Fernie 1983) in contrast with the excellent  $(RI)_C$  system defined by Cousins. Accurate photometry is available from Eggen (1979) who observed this star in the Eggen-Kron  $(RI)_K$  system defined by Eggen (1968, 1975). An excellent repre-

sentation of this system is available from Weis (1983, 1996) for which accurate transformations to the Johnson-Cousins system are given by Bessell (1995). Adopting this transformation, we obtain the following composite magnitudes ( $V = 5.75$ ,  $V - R_C = 0.34$ ,  $(R - I)_C = 0.42$ ) from which the magnitudes of the primary in different colours ( $m_A$ ) can be calculated using the following equation:<sup>5</sup>

$$m_A = m + 2.5 \log(1 + 10^{-0.4 \Delta m}), \quad (4)$$

where  $\Delta m$  is the differential photometry in the given colour. By doing so we obtain the magnitudes and colours of the primary listed in Table 3 from which  $T_{\text{eff}} = 5730 \pm 340$  K,  $M_{\text{Bol}} = 5.27 \pm 0.05$  mag and  $R = 0.80 \pm 0.09 R_\odot$ . The effective temperature and linear radius are now in much better agreement with other determinations. The striking difference of these parameters with respect to the previous values (though the errors are still similar) is likely to be due to the shift in the zero-points when the right photometric system is adopted. The errors are still large, but that is mostly due to the uncertainties in  $\Delta m$  that are of the order of 0.3 mag.

For this star we obtain a mass practically identical to the empirical measured one and a rather low helium content, although the errors in both empirical and theoretical mass determinations are unfortunately very large. Interestingly Fernandes et al. (1998) could not calibrate stellar models to this system unless by assuming extremely low helium abundance  $Y < 0.2$  and high age ( $> 20$  Gyr) both at odds with cosmological constraints. In our case the problem is somehow reduced, but not solved. Fernandes et al. (2002) were finally able to calibrate a stellar model including diffusion with a reasonable age (9.3 Gyr) and helium content ( $Y = 0.253$ ) however only by assuming an initial metallicity  $[\text{Fe}/\text{H}] = -0.185 \pm 0.054$  i.e. almost 0.4 dex higher than their adopted observed metallicity ( $[\text{Fe}/\text{H}] = -0.57 \pm 0.11$ ). Such a difference of  $\sim 0.4$  dex would imply a huge effect of diffusion that is supported neither by observations (see discussion in Section 5) nor by theoretical modeling: for this object D'Antona et al. (2005b), assuming an age of 12 Gyr such as to maximize the effect, found a difference of 0.12 dex due to metal diffusion. Furthermore, their adopted observed metallicity is 0.3 dex higher than the most recent determinations ( $[\text{Fe}/\text{H}] = -0.90$ , see above), a difference that not even NLTE can easily explain.

## 6.8 $\mu$ Cas A

Another interesting metal poor system is the halo binary  $\mu$  Cas (HD 6582) which, from the pioneering work of Dennis (1965), has been extensively studied for its potential role in determining the primordial helium abundance (e.g. Catchpole, Pagel & Powell 1967, Hegyi & Curott 1970, Haywood, Hegyi & Gudehus 1992). These older works had to deal with much less accurate estimates of mass, luminosity, temperature, metallicity and pre-*Hipparcos* parallax so that

<sup>5</sup> As a further consistency check of our procedure, we point out that the composite  $(V - I) = 0.96$  given by ten Brummelaar et al. (2000) can be transformed to the Cousins system with the recent calibration given by An et al. (2007) in their appendix A. Such a transformation returns  $V - I_C = 0.76$ , identical to what we obtain.

they estimated helium abundances ranging from 0 (Hegyi & Crotti, 1970) to 0.4 (Catchpole et al. 1967) with a preference around 0.2 (Haywood et al. 1992). While the high magnitude difference between the two components in the optical ( $\Delta m_v = 5.5$ , McCarthy et al. 1993) has for a long time hindered accurate relative angular separation measurements and therefore precise mass determinations, the huge luminosity difference makes almost negligible the contribution of the secondary to optical photometry. According to McCarthy et al. (1993),  $\Delta m = 5.5 \pm 0.7$  at  $0.55 \mu\text{m}$  (roughly  $V$  band) and decreases to  $\Delta m = 4.5 \pm 1.0$  at  $0.75 \mu\text{m}$  (roughly  $I$  band). Using equation (4) we can estimate the contribution of the secondary in  $V$  band to be only 0.007 mag, whereas increases to 0.017 mag in  $I$  band. We only study the primary component. We have taken the mean composite Johnson  $BV$  magnitudes found in the General Catalogue of Photometric Data (Mermilliod, Mermilliod & Hauck 1997) and  $RI_K$  magnitudes from Eggen (1973) then converted to the standard Cousins system with the transformation given in Bessell (1995).  $V(RI)_C$  magnitudes have then been corrected according to equation (4) to account for the contribution of the secondary. Although the corrections are at the same level of the photometric accuracy, they avoid the introduction of systematics in the zero-point. The magnitude difference between the two components in  $B$  band is not available, but in this band the contribution of the cool secondary component is certainly below a few millimag. We have used the *Hipparcos* parallax and for the metallicity we have taken the mean value from six recent determinations (Luck & Heiter 2006, Mishenina et al. 2004, Allende Prieto et al. 2004, Fuhrmann 2004, Gratton et al. 2003, Fulbright 2000). All determinations agree remarkably well, with  $[\text{Fe}/\text{H}] = -0.91 \pm 0.05$  dex and  $[\alpha/\text{Fe}] = 0.36 \pm 0.04$  dex. The determination of the empirical masses of both components has been troublesome because of the aforementioned luminosity difference, however the most recent data agree and we use the Drummond, Christou & Fugate (1995) mass of the primary  $0.742 \pm 0.059 M_\odot$  that becomes  $0.757 \pm 0.059 M_\odot$  after accounting for the better parallax provided by *Hipparcos* (Lebreton et al. 1999).

We obtain a mass a little more than  $1\sigma$  higher than the empirical value. Again, we keep temperature as a free parameter to investigate by how much it should change to exactly reproduce the observed mass. In this case an increase of 175 K in the effective temperature would be enough to reduce the mass to the observed value and to increase the helium abundance to  $Y = 0.255$ . Thévenin & Idiart (1999) found a correction of +0.15 dex for the metallicity of this star because of NLTE effects. An increase of the metallicity by such an amount changes its mass to  $0.828 M_\odot$  and  $Y = 0.205$ , but to exactly recover the measured mass,  $T_{\text{eff}}$  should be still increased by 145 K, implying a helium abundance  $Y = 0.273$ , higher than the solar value.

## 6.9 What we learn from binaries

The comparison between empirical and isochrone masses for the stars previously studied is shown in Figure 10. Notice that neither component of  $\xi$  Boo is included in the comparison.

The overall agreement is very good and there is only one star (HD 195987 A) that is off by  $3\sigma$ . Also, the fit pivots

around  $0.6 - 0.7 M_\odot$  and below  $\sim 0.9 M_\odot$  it is close to the one-to-one relation, with a difference of at most  $0.03 - 0.04 M_\odot$ . The fit diverges from the one-to-one relation when going at higher masses because of possible evolutionary effect associated with vB22 A and HD 195987 A, as we have already discussed. If these two objects are neglected, the fit is in outstanding agreement with the one-to-one relation (Figure 10).

When the difference between measured and predicted masses is shown as function of metallicity however, it appears that the most serious discrepancies arise at low metallicity (half solar and lower). Such differences have been extensively discussed throughout the Section and in its most simple investigation, a conciliation with the empirical masses would require a change in the measured metallicities or a cooling of the isochrones or both of them.

In the case of HD 195987, a closer agreement with the empirical masses could be achieved by cooling the isochrones by a different amount for the two components, but their helium content would then be very different.

In the case of  $\eta$  Cas B the mass predicted is lower than the measured one and cooling the isochrones to improve the mass would even decrease the helium abundance.

85 Peg A is in very good agreement with the empirical mass and has a rather low helium content, but the errors are unfortunately large.

Finally in the case of  $\mu$  Cas A, diffusion and NLTE effects might solve the problem, but the implied helium content would then be higher than the solar one.

A thorough investigation would require to simultaneously change temperature, luminosity and metallicity to find the set of solutions that better fit the empirical masses. However, here we are not searching for the set of parameters that better fits the data, but rather testing the applicability range of our results. For metallicity above the solar one the agreement is always within  $1\sigma$  and this strengthens the conclusion we already reached in Section 4. At low metallicity, in spite of the large uncertainties of the individual determinations, the occurrence of very low  $Y$  values, well below the consensus primordial level, is also confirmed, most likely indicating inadequacies of extant low Main Sequence, metal poor stellar models.

Also, it is clear from Figure 10 that at low metallicities isochrones tend to overestimate masses; a decrease of the masses would actually imply a higher helium content (Figure 4). The use of isochrones as old as 10 Gyr could reduce the discrepancy in mass by at most  $\sim 0.03 M_\odot$  and therefore the scatter at low  $Z$  would still be present. As we have already said there is no neat relation between age and metallicities and 5 Gyr old isochrones are representative of the mean age of disk stars. Besides, the use of older isochrones would only improve the agreement in mass, leaving practically unchanged the anomalously low helium abundances in these stars.

## 7 MASS-LUMINOSITY RELATION

In the previous Section we have compared the masses deduced from the isochrones to those directly measured for a congruous set of binary stars. Another approach is to compare empirical mass-luminosity relations to the theoretical

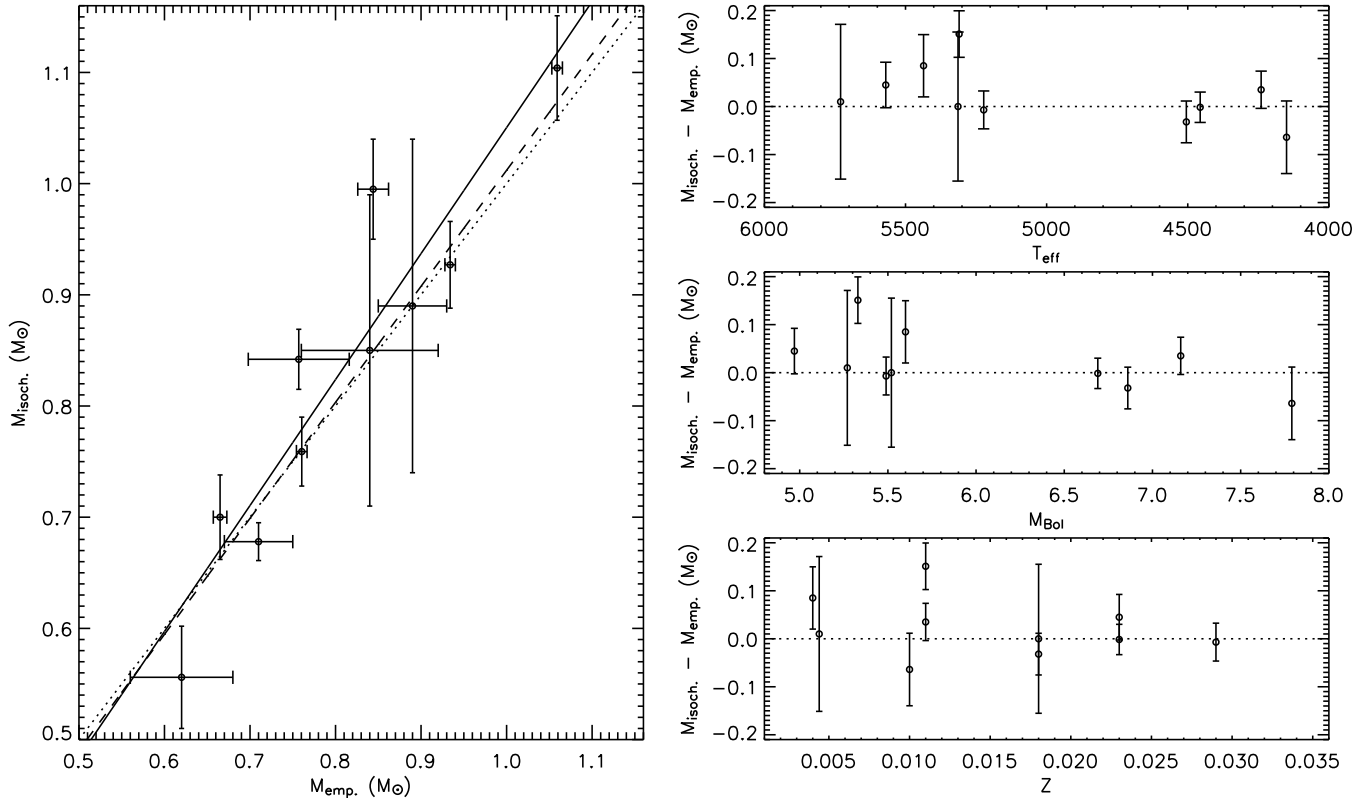


**Figure 10.** Empirical vs isochrones' masses for the binaries studied in Section 6. Dotted lines are the 1-to-1 relation intended to guide the eye. The continuous line is the fit of the empirical vs. isochrones' masses; the dashed line is the same fit, when the two possibly evolved stars vB22 A and HD 195987 A are excluded.

masses (i.e. deduced from the isochrones) and the empirical luminosities available for our 86 stars of Section 2 (Figure 11).

For the comparison we use the empirical mass-luminosity relation of Henry & McCarthy (1993) which extends from  $1M_{\odot}$  down to  $0.08M_{\odot}$ . Recent improvements of this relations (e.g. Henry et al. 1999; Delfosse et al. 2000) only concern the low mass regime that is of no interest for the purpose of the present investigation. The Henry & McCarthy (1993) relation is given in the infrared ( $J, H, K$ ) and visible ( $V$ ) bands. Since most of the infrared photometry used by Henry & McCarthy (1993) is in the CIT system, we have converted our 2MASS colours according to the transformation given in Carpenter (2001). The corrections are typically of a few 0.01 magnitudes, whereas the larger uncertainties in the empirical relations actually come from the 0.03-0.06 scatter in  $\log(M/M_{\odot})$ . Another empirical mass-luminosity relation in  $V$  band is that of Kroupa, Tout & Gilmore (1993) who followed a different approach to derive it. Rather than fit the data directly, Kroupa et al. (1993) adopted a reference luminosity function, and chose a functional form for the mass function. The mass- $M_V$  relation was then varied to give the lowest residuals with respect to the observed data points.

The comparison between our data and empirical mass-luminosity relations is shown in Figure 11. Overall, the agreement is quite good and the data actually follow the trend defined by the Henry & McCarthy (1993) relations.

In the infrared, the points slightly depart from the empirical formulae at brighter luminosities and masses higher than  $\sim 0.85M_{\odot}$  (depending on the band). This might be due to evolutionary effects, however we caution that the Henry & McCarthy (1993) formulae are rather noisy; interestingly, when the single stars used by Henry & McCarthy (1993) are overplotted (from their table 5), at higher masses the agreement is good. Therefore, considering the uncertainty in the data and the scatter in the empirical relations, the agreement is within  $1\sigma$  throughout the entire range. Also, the Henry & McCarthy (1993) mass-luminosity relation is obtained using stars of intermediate disk age with various metallicities so that either of these effects are built in the relations themselves. We also show the relations of Delfosse et al. (2000) (valid for  $M_K \geq 4.5$ ) and Kroupa et al. (1993) in the visible. In  $V$  band the scatter is much larger, but there is no clear departure from the empirical relations: stars with different metallicities lie in different parts of the mass-luminosity relation whereas the distribution is blurred in the infrared. This metallicity dependence is also confirmed when the empirical binary data of Table 3 are overplotted. Such a behaviour is predicted by all theoretical models (e.g. Chabrier & Baraffe 2000) and it was also noticed by Delfosse et al. (2000) for stars with masses lower than those covered in the present study.

Interestingly, in Figure 11 a linear fit for the stars of Section 2 with  $Z < 0.006$  (thin blue line) and with  $Z \geq 0.022$  (thin red line) shows a marked difference in the

**Table 3.** Magnitudes and colours adopted and  $T_{eff}$  and  $M_{Bol}$  recovered according to the procedure described in Section 2. Helium abundances and masses recovered from the isochrones according to the procedure described in Section 4 are compared to the masses empirically measured. Notice that  $\xi$  Boo is discarded from the comparison for the reason explained in Section 6.4. The isochrones used are 5 Gyr old, except for vB22 A for which a 500 Myr isochrones have been chosen.

HD	Name	$V$	$B - V$	$V - R_C$	$(R - I)_C$	$V - H$	$V - K_S$	$T_{eff}$ (K)	$M_{Bol}$	$Z$ (measured)	$Y$	$\frac{M}{M_\odot}$	$\frac{M}{M_\odot}$ (measured)
128621	$\alpha$ Cen B	1.340	0.839	0.474	0.404			5223 $\pm$ 58	5.49 $\pm$ 0.03	0.029 $\pm$ 0.002	0.263 $\pm$ 0.028	0.927 $\pm$ 0.039	0.934 $\pm$ 0.0061
27130 A	vB22 A	8.443	0.713	0.392	0.358			5570 $\pm$ 56	4.97 $\pm$ 0.05	0.023 $\pm$ 0.002	0.216 $\pm$ 0.028	1.104 $\pm$ 0.047	1.0591 $\pm$ 0.0062
27130 B	vB22 B	10.74	1.19	0.75	0.62			4456 $\pm$ 43	6.69 $\pm$ 0.06	0.023 $\pm$ 0.002	0.232 $\pm$ 0.021	0.759 $\pm$ 0.031	0.7605 $\pm$ 0.0062
165341 A	70 Oph A	4.21	0.86		0.37			5314 $\pm$ 240	5.52 $\pm$ 0.11	0.018 $\pm$ 0.003	0.252 $\pm$ 0.091	0.89 $\pm$ 0.15	0.89 $\pm$ 0.04
165341 B	70 Oph B	6.00	1.15		0.59			4505 $\pm$ 37	6.86 $\pm$ 0.04	0.018 $\pm$ 0.003	0.262 $\pm$ 0.022	0.678 $\pm$ 0.017	0.71 $\pm$ 0.04
131156 A	$\xi$ Boo A	4.70	0.73		0.39			5404 $\pm$ 120	5.38 $\pm$ 0.06	0.011 $\pm$ 0.002	0.185 $\pm$ 0.065	0.923 $\pm$ 0.066	0.86 $\pm$ 0.07
131156 B	$\xi$ Boo B	6.97	1.16		0.58			4493 $\pm$ 40	7.22 $\pm$ 0.04	0.011 $\pm$ 0.002	0.273 $\pm$ 0.022	0.587 $\pm$ 0.017	0.70 $\pm$ 0.05
195987 A		7.19				1.827	1.889	5310 $\pm$ 40	5.33 $\pm$ 0.03	0.011 $\pm$ 0.006	0.123 $\pm$ 0.066	0.995 $\pm$ 0.045	0.844 $\pm$ 0.018
195987 B		9.59				3.068	3.232	4240 $\pm$ 20	7.16 $\pm$ 0.09	0.011 $\pm$ 0.006	0.129 $\pm$ 0.062	0.700 $\pm$ 0.038	0.6650 $\pm$ 0.0079
4614 B	$\eta$ Cas B	7.51	1.39		0.76			4150 $\pm$ 130	7.79 $\pm$ 0.11	0.010 $\pm$ 0.002	0.190 $\pm$ 0.057	0.556 $\pm$ 0.046	0.620 $\pm$ 0.060
224930 A	85 Peg A	5.81		0.31	0.39			5730 $\pm$ 340	5.27 $\pm$ 0.05	0.0044 $\pm$ 0.0006	0.21 $\pm$ 0.13	0.85 $\pm$ 0.14	0.84 $\pm$ 0.08
6582 A	$\mu$ Cas A	5.170	0.694	0.400	0.274			5436 $\pm$ 44	5.60 $\pm$ 0.02	0.0040 $\pm$ 0.0005	0.172 $\pm$ 0.028	0.842 $\pm$ 0.027	0.757 $\pm$ 0.059

Error in  $M_{Bol}$  also account for the uncertainty in parallaxes. Errors in parallaxes are always better than 1.8% and for most of the stars are of order  $\sim 0.5\%$ . Labels A and B indicate the primary and the secondary, respectively.

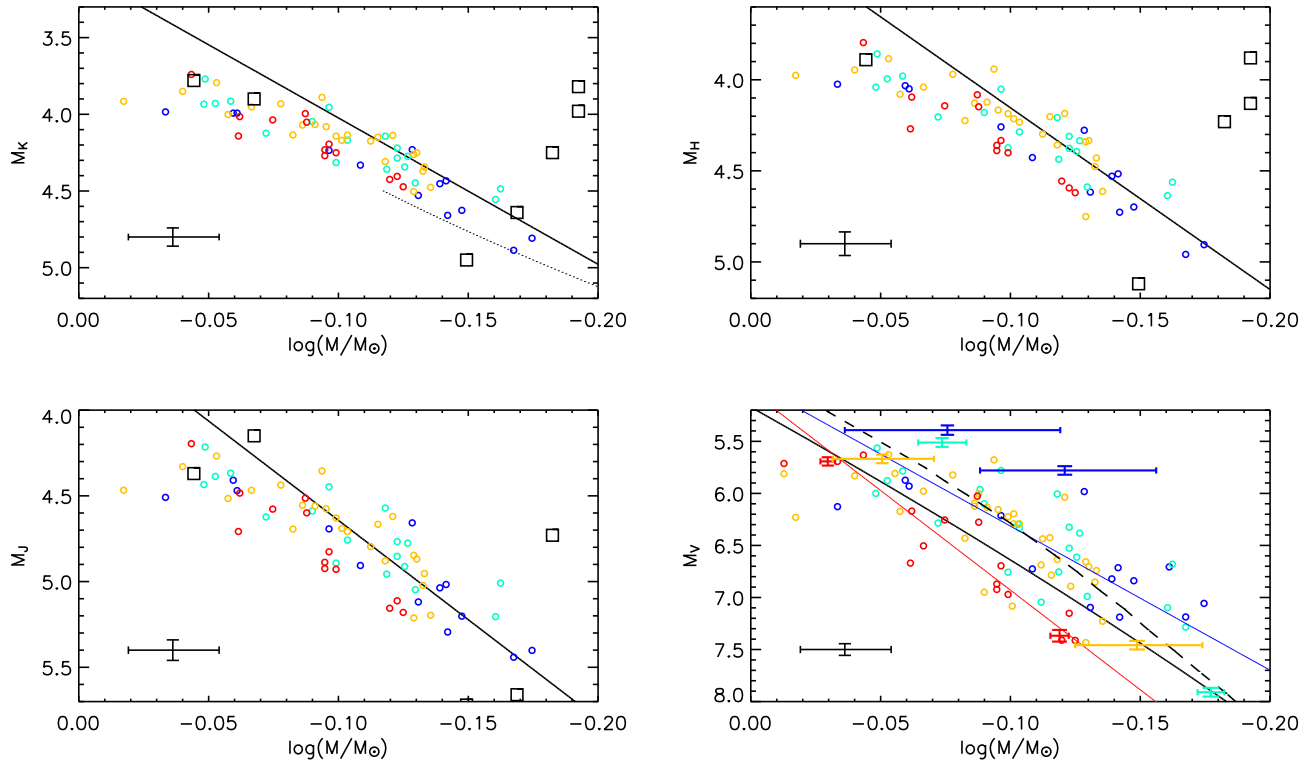


**Figure 11.** Empirical mass-luminosity relation from Henry & McCarthy (1993) in different bands (solid black line) overplotted to our sample stars. The squares are the stars used by Henry & McCarthy (1993) to fit their empirical mass-luminosity relation. Infrared colours have been converted to the CIT system. Only stars with accurate IR photometry (“j.”+“h.”+“k\_msicom”<0.10) are shown. Points correspond to the sample stars in the range  $Z < 0.006$  (blue),  $0.006 \leq Z < 0.012$  (cyan),  $0.012 \leq Z < 0.022$  (yellow),  $Z \geq 0.022$  (red). The dotted line in the first panel is the Delfosse et al. (2000) empirical relation. The dashed line in the fourth panel is the Kroupa et al. (1993) empirical relation. In the fourth panel are also shown (with colored error bars) the stars of Table 3 with the exception of  $\xi$  Boo A and B (see discussion in Section 6), vB22 A and  $\eta$  Cas B (outside of the plot range). The thin red and blue lines are fits to the sample stars as explained in the text. A typical error bar for the points is also shown in the lower left of each panel.

slope, whereas the empirical relation of Henry & McCarthy (1993) is somewhat between the two. Indeed, more empirical masses and luminosities for metal poor binaries would be extremely interestingly. If a steeper slope for metal poor stars is required, that could be achieved by reducing the mass deduced from the isochrones that in turn would imply a higher helium abundance (see Figure 4). Therefore we suggest that more data on the empirical mass-luminosity relation for metal poor stars could help to constrain the helium abundance in stars.

## 8 THE HELIUM CONTENT IN PLANET HOST STARS

Stars with planetary companions have been shown to be, on average, considerably more metal-rich when compared with stars without planets in the solar neighborhood (e.g. Gonzalez 1997, 1998; Santos, Israelian & Mayor 2000; Gonzalez et al. 2001; Santos et al. 2005; Fischer & Valenti 2005). A high degree of statistical significance is obtained when iron is used as the reference element. When other elements are investigated, the situation is much less clear (see e.g. Gonzalez 2003, 2006 for reviews). There is some evidence that planet

host stars differ from other nearby stars without planets in their abundances of Mg, Al, Si, V, Co and Ni. As regards the light elements, no significant difference between planet and non planet host stars is found for Be (e.g. Santos et al. 2004) whereas the situation is more uncertain for Li (e.g. Gonzalez 2006).

Here we attempt for the first time to derive the helium abundance for a small set of planet host stars. They all have metallicities around or above the solar one, where the isochrones have been proven to be in overall good agreement with the empirical data (see Section 6 and 7).

Our sample of planet host stars is drawn from the comprehensive list of Santos et al. (2004) which provides accurate spectroscopic [Fe/H] measurements. Abundances for the  $\alpha$ -elements are available from the same research group (Gilli et al. 2006). Two planet host stars (HD3651 and HD130322) were in our original sample of Section 2. The other stars have been chosen if accurate  $BV(RI)_C$  colours (from Bessell 1990) were available so that  $T_{eff}$  and bolometric luminosities could be estimated as described in Section 2. If accurate  $JHK_S$  magnitudes were also available from the 2MASS, the IRFM (Casagrande et al. 2006) has been applied directly. We also used the *Hipparcos* classification to discard any variable star. The absence of vari-

ability ensures that the stars are likely to be chromospherically quiet so that chromospheric-age relations can be safely used (Donahue 1998). Most of the planet host stars for which we found accurate metallicities and photometry have in fact  $M_{Bol} < 5.4$  meaning that evolutionary effects need to be taken into account. For all these stars, age determinations based on chromospheric indices are available from Saffe, Gómez & Chavero (2005). Two calibrations are usually adopted to deduce ages from chromospheric indices: that of Donahue (1993) and that of Rocha-Pinto & Maciel (1998). For a number of reasons, the Donahue (1993) calibration is usually preferred (Feltzing et al. 2001; Saffe et al. 2005) and is adopted here.

The chromospheric-age relation is considered to be rather robust for ages younger than  $\sim 6$  Gyr (Saffe et al. 2005). When long-term observations are available, for a given functional form, the age uncertainty can be as small as  $\sim 1$  Gyr (Donahue 1998). More serious problems come if a star is actually in a Maunder-minimum state where errors estimates can be as high as 5 Gyr. However there are indications that Maunder-minima are very rare among young stars (e.g. Gustafsson 1999). In our case, planet host stars have a median age of 5.1 Gyr using the Donahue (1993) calibration, consistently with the evidence that most of the nearby solar-type stars have activity level and age similar to the Sun (Henry et al. 1996). Their chromospheric indices are averaged over years of observations (Saffe et al. 2005) and we are still working in a rather low luminosity area of the HR diagram, where isochrones of different ages do not differ by much. For stars with  $M_{Bol} < 5.4$  a variation of 1 Gyr changes masses by  $0.04 - 0.05 M_{\odot}$  and helium abundances  $Y$  by 0.02-0.03 on average, i.e. on the same order of the uncertainties originating from the errors in  $T_{eff}$  and  $M_{Bol}$ . The complete list of planet host stars with their relevant parameters is shown in Table 3.

Our results suggest that within the present day accuracy, planet host stars do not show any anomalous helium abundance with respect to other field stars. This is in agreement with the fact that  $Y_{\odot}$  is recovered within  $1\sigma$  from field stars (Table 2). A Kolmogorov-Smirnov test for the helium content between stars with and without planets in the same metallicity range of Table 3 confirm that the two populations are drawn from the same distribution. The number of available data points is still small, with large errorbars; but we expect that in the near future, studies of planet host stars in the Lower Main Sequence will improve on the robustness of this conclusion.

Most of the studies about exoplanets depend quite strongly on the physical properties (mostly radius and mass) of the planet host stars. Such properties are usually obtained from the isochrones. In this study we have proven that at high metallicity the isochrones can be used with a certain confidence. When our masses are compared to those obtained by Santos et al. (2004) interpolating isochrones with standard helium abundances, the agreement is usually good with a mean difference  $\Delta M = 0.04 \pm 0.14 M_{\odot}$ .

## 9 CONCLUSIONS

In this work we have compared a large set of K dwarfs to theoretical isochrones with different helium content and metal-

licity in order to determine the helium-to-metal enrichment ratio  $\Delta Y/\Delta Z$  in the Solar Neighbourhood.

For all our stars the fundamental physical parameters were derived empirically and homogeneously, with the specific aim of measuring small differential effects along the Lower Main Sequence (Section 2). The isochrones used are among the most up-to-date, they implement the latest input physics and cover a large grid of  $(Y, Z)$  values; also, we have verified that, for similar  $(Y, Z)$  content they compare very well to other recent sets (Yonsei-Yale, Teramo and MacDonald) and therefore our results do not depend significantly on the specific isochrones employed. The size and homogeneity of the sample of stars, the accuracy in both empirical and theoretical data, together with the possibility of making the comparison directly in the  $T_{eff} - M_{Bol}$  plane, where the effect of the helium content are most evident, are the major improvements over similar work in the past.

At metallicities around and above the solar, we obtain  $\Delta Y/\Delta Z = 2.2 \pm 1.1$ , but when considering lower metallicities, surprisingly, we have found that the difference in the location of the metal rich and metal poor Main Sequence is less than expected (Section 3). As a consequence, theoretical isochrones can fit metal poor stars only by assuming *very low helium abundances*, well below the primordial Big-Bang value (Section 4; Figure 5). This result is quite puzzling.

The discrepancy was noticed before (Lebreton et al. 1999), but with the present, much larger sample the trend is systematic and very significant. Lebreton et al. (1999) showed that improvements in stellar models (diffusion) and observations (NLTE effects) could help in solving the problem, although their conclusions were based on a rather small number of stars. In fact, Salaris et al. (2000) pointed out that with the accuracy and the size of the sample available at the time, the improvement obtained with diffusive stellar models was not very significant. The study of enlarged samples was also advocated by Lebreton (2000). The present study reinforces the evidence of the discrepancy and we find that diffusion and NLTE are unlikely to solve the problem completely. Extremely low helium abundances can be avoided if the mixing-length steadily decreases with metallicity for  $Z$  below solar, but this is a major change to make to stellar models.

Interestingly, discrepancies between theory and observations for stars less massive than the Sun have already been reported in the literature from the studies of binaries (e.g. Popper 1997, Torres & Ribas 2002, see Section 6). However, such discrepancies in the range of K dwarfs have not yet caught – in our opinion – the attention they deserve, as most of the studies aiming to empirically measure mass-luminosity relations have preferentially focused on either earlier or later spectral types. We urge stellar model makers to reassess the modeling of low metallicity, lower main sequence stars.

As we have discussed in Section 6, accurate masses and fundamental physical parameters for metal poor dwarf binaries would be a powerful test of stellar models. The slope of the mass-luminosity relation in the metal poor regime could directly test the effect of diffusion (Section 5) and be used to determine the helium abundance (Section 7). Low degree modes from space-based asteroseismology missions can be used to determine the helium abundance in stellar envelopes with an accuracy of 0.03 for a  $0.8 M_{\odot}$  star (Basu et

**Table 3.** Physical parameters and ages adopted for planet host stars and helium abundances and masses deduced from the isochrones.

HD	$T_{eff}$	$M_{bol}$	$Z$	Age (Gyr)	$Y$	$\frac{M}{M_\odot}$
142	$6247 \pm 81$	$3.63 \pm 0.05$	$0.024 \pm 0.004$	5.93	0.29	1.09
3651	$5191 \pm 158$	$5.47 \pm 0.07$	$0.022 \pm 0.002$	5.13	0.21	0.98
17051	$6067 \pm 123$	$4.19 \pm 0.05$	$0.028 \pm 0.004$	1.47	0.27	1.19
70642	$5667 \pm 60$	$4.81 \pm 0.04$	$0.027 \pm 0.002$	3.88	0.26	1.04
130322	$5429 \pm 31$	$5.54 \pm 0.10$	$0.017 \pm 0.002$	1.24	0.25	0.86
160691	$5689 \pm 46$	$4.13 \pm 0.04$	$0.032 \pm 0.003$	6.41	0.29	1.10
179949	$6205 \pm 104$	$4.07 \pm 0.05$	$0.025 \pm 0.003$	2.05	0.30	1.12
210277	$5556 \pm 77$	$4.79 \pm 0.04$	$0.027 \pm 0.003$	6.93	0.30	0.93

The uncertainty in mass and helium abundance for stars with  $M_{bol} < 5.4$  is not straightforward to determine, since age plays a role. However, as we discuss in the text, the uncertainty due to age determinations is of the same order of that due to the uncertainties in the other physical parameters. In this case, a typical uncertainty of  $\pm 0.1$  in masses and  $\pm 0.05$  in helium abundances is a reasonable choice. Errors in  $M_{bol}$  also account for the uncertainty in parallaxes.

al. 2004). Such accuracy is comparable to that in the present work. The study of such modes in metal poor dwarfs with on-going or forthcoming space missions like *COROT* and *Kepler* is therefore needed.

Theoretical isochrones are also extensively used to determine the distance scale fitting the observed colour-magnitude diagram of globular clusters. Metal poor isochrones with primordial, or close to primordial, helium abundance are used to infer their distance. However, our direct observations of nearby stars are challenging low metallicity isochrones : if extremely helium poor isochrones are formally needed to fit empirical data, this would stretch the distance scale by 0.1 – 0.2 magnitudes. Besides, assuming primordial helium for the metal poor population in such objects would imply, in a differential sense, extremely helium enhanced values for the metal rich counterparts. We stress that here we are not arguing that such extremely low helium abundances are real; rather they are likely to stem from current limits in stellar models. Clearly direct parallaxes measurements for stars in globular clusters (as *Gaia* and *SIM* will provide) will shed new light on the problem. The accurate distances to the Hyades by *Hipparcos* have already posed a lot of questions on their helium content.

In the meanwhile, more studies for modeling low mass, metal poor stars are needed. Actually new abundance determinations from 3D model atmospheres are revolutionizing the field and the solar model itself is under profound revision, so that in coming years we expect many exciting breakthroughs.

Our study also shows that at metallicities around and above the solar one, theoretical models are in good agreement with observations. This is important in studies of exoplanets, since they still heavily depend on theoretical models to put some constraints on the properties of the parent star. It also shows that, in the high metallicity regime our result of  $\Delta Y/\Delta Z = 2.2 \pm 1.1$  is rather reliable and we plan to discuss it further by means of galactic chemical evolution models.

## ACKNOWLEDGMENTS

LC acknowledges the hospitality of the Department of Astronomy at the University of Pennsylvania, the Research School of Astronomy and Astrophysics at Mount Stromlo,

the University of Padova and the Osservatorio Astronomico di Padova, where part of this work was carried out. LC also acknowledges the Finnish Graduate School in Astronomy and Space Physics and the Turku University Foundation for financial support. This study was funded also by the Academy of Finland (CF) and by the 6<sup>th</sup> Framework Program of the European Communities (Marie Curie Fellowship nr. MEIF-CT-2005-010884; LP). This research has made use of the the General Catalogue of Photometric Data operated at the University of Lausanne and the SIMBAD database, operated at CDS, Strasbourg, France. This publication makes use of data products from the Two Micron All Sky Survey, which is a joint project of the University of Massachusetts and the Infrared Processing and Analysis Center/California Institute of Technology, funded by the National Aeronautics and Space Administration and the National Science Foundation.

## REFERENCES

- Allende Prieto C., Lambert D.L., 1999, A&A, 352, 555
- Allende Prieto C., García López R., Lambert D.L., Gustafsson B., 1999, ApJ, 527, 879
- Allende Prieto C., Barklem P.S., Lambert D.L., Cunha K., 2004, A&A, 420, 183
- Alonso A., Arribas S., Martínez-Roger C., 1995, A&A, 297, 197
- Alonso A., Arribas S., Martínez-Roger C., 1996a, A&A, 117, 227
- Alonso A., Arribas S., Martínez-Roger C., 1996b, A&A, 313, 873
- An D., Terndrup D.M., Pinsonneault M.H., Paulson D.B., Hanson R.B., Stauffer J.T., 2007, ApJ, 655, 233
- Andersen J., 1991, A&AR, 3, 91
- Antia H.M., Basu S., 2005, ApJ, 620, 129
- Asplund M., 2005, ARA&A, 43, 481
- Asplund M., Grevesse N., Sauval A.J., 2005, in Barnes T.G., III, Bash F. N., eds, ASP Conf. Ser. Vol. 336, Cosmic Abundances as Records of Stellar Evolution and Nucleosynthesis., p.25
- Asplund M., Lambert D.L., Nissen P.E., Primas F., Smith V.V., 2006, ApJ, 644, 229
- Bahcall J.N., Pinsonneault M.H., Wasserburg G.J., Rev Mod Phys, 67, 781

Bahcall J.N., Pinsonneault M.H., Basu S., Christensen-Dalsgaard J., 1997, *Phys.Rev.Lett.*, 78, 171

Bahcall J.N. Serenelli A.M., Basu S., 2006, *ApJS*, 165, 400

Baliunas S.L. et al., 1995, *ApJ*, 438, 269

Basu S., Antia H.M., 2004, *ApJ*, 606, 85

Basu S., Pinsonneault M.H., Bahcall J.N., 2000, *ApJ*, 529, 1084

Basu S., Mazumdar A., Antia H.M., Demarque P., 2004, *MNRAS*, 350, 277

Bedin L.R., Piotto G., Anderson J., Cassisi S., King I.R., Momany Y., Carraro G., 2004, *ApJ*, 605, 125

Bessell M. S., 1979, *PASP*, 91, 589

Bessell M. S., 1990, *A&AS*, 83, 357

Bessell M. S., 1995, *PASP*, 107, 672

Bessell M. S., 2000, *PASP*, 112, 961

Bigot L., Kervella P., Thévenin F., Ségransan D., 2006, *A&A*, 446, 635

Boden A.F., Torres G., Latham D.W., 2006, *ApJ*, 644, 1193

Bonfils X., Delfosse X., Udry S., Santos N.C., Forveille T., Ségransan D., 2005, *A&A*, 442, 635

Bonifacio et al., 2007, *A&A*, 462, 851

Bressan A., Fagotto F., Bertelli G., Chiosi C., 1993, *A&AS*, 100, 647

Brown A.G.A., Arenou F., van Leeuwen F., Lindegren L., Luri X., 1997, *Hipparcos - Venice 1997 Proc.*, ESA SP-402. ESA Publications Division, Noordwijk, p.63

Brun A.S., Turck-Chièze S., Zahn J.P., 1999, *ApJ*, 525, 1032

Caloi V., D'Antona F., 2007, *A&A*, 463, 949

Carpenter J.M., 2001, *AJ*, 121, 2851

Carrier F., Eggenberger P., 2006, *A&A*, 450, 695

Casagrande L., Portinari L., Flynn C., 2006, *MNRAS*, 373, 13

Castellani V., Ciacio F., degl'Innocenti S., Fiorentini G., 1997, *A&A*, 322, 801

Castellani V., degl'Innocenti S., Marconi M., 1999, *A&A*, 349, 834

Catchpole R.M., Pagel B.E.J., Powell A.L.T., 1967, *MNRAS*, 136, 403

Chaboyer B., Demarque P., 1994, *ApJ*, 433, 510

Chaboyer B., Deliyannis C.P., Demarque P., Pinsonneault M.H., Sarajedini A., 1992, *ApJ*, 388, 372

Chaboyer B., Fenton W.H., Nelan J.E., Patnaude D.J., Simon F.E., 2001, *ApJ*, 562, 521

Chabrier G., Baraffe I., 2000, *ARA&A*, 38, 337

Chiappini C., Renda A., Matteucci F., 2002, *A&A* 395, 789

Chieffi A., Straniero O., Salaris M., 1995, *ApJ*, 445, 39

Chiosi C., Matteucci F., 1982, *A&A*, 105, 140

Cordier D., Pietrinferni A., Cassisi S., Salaris M., 2007, *AJ*, 133, 468

Cox J.P., Giuli R.T., 1968, *Principles of Stellar Structure*. Gordon & Breach, New York

Christensen-Dalsgaard J., Proffitt C.R., Thompson M.J., 1993, *ApJ*, 403, 75

D'Antona F., Bellazzini M., Caloi V., Pecci F.F., Galleti S., Rood R.T., 2005a, *ApJ*, 631, 868

D'Antona F., Cardini D., Di Mauro M.P., Maceroni C., Mazzitelli I., Montalbán J., 2005b, *MNRAS*, 363, 847

de Bruijne J.H.J., Hoogerwerf R., de Zeeuw P.T., 2001, *A&A*, 367, 111

Delfosse X., Forveille T., Ségransan D., Beuzit J.-L., Udry S., Perrier C., Mayor M., 2000, *A&A*, 364, 217

Deliyannis C.P., Demarque P., 1991, *ApJ*, 370, 89

Demarque P., Woo J.-H., Kim Y.-C., Yi S.K., 2004, *ApJS*, 155, 667

Dennis T.R., 1965, *PASP*, 77, 283

Donahue R.A., 1993, Ph.D. Thesis, New Mexico State University

Donahue R.A., 1998, in *Stellar Systems and the Sun*, ed. R.A. Donahue, & J. A. Bookbinder, *ASP Conf. Ser.*, 154, 1235

Drummond J.D., Christou J.C., Fugate R.Q., 1995, *ApJ*, 450, 380

Edmonds P., Cram L., Demarque P., Guenther D.B., Pinsonneault M.H., 1992, *ApJ*, 394, 313

Eggen O.J., 1968, *Roy. Obs. Bull.*, No. 137

Eggen O.J., 1973, *ApJ*, 182, 821

Eggen O.J., 1975, *PASP*, 87, 107

Eggen O.J., 1979, *ApJS*, 39, 89

Eggenberger P., Charbonnel C., Talon S., Meynet G., Maeder A., Carrier F., Bourban G., 2004, *A&A*, 417, 235

Fabricius C., Makarov V.V., *A&A*, 356, 141

Faulkner J., 1967, *ApJ*, 147, 617

Feltzing S., Gonzalez G., 2001, *A&A*, 367, 253

Feltzing S., Holmberg J., Hurley J.R., 2001, *A&A*, 377, 911

Fernandes J., Neuforge C., 1995, *A&A*, 295, 678

Fernandes J., Lebreton Y., Baglin A., 1996, *A&A*, 311, 127

Fernandes J., Lebreton Y., Baglin A., Morel P., 1998, *A&A*, 338, 455

Fernandes J., Morel P., Lebreton Y., 2002, *A&A*, 392, 529

Fernie J.D., 1983, *PASP*, 95, 782

Ferraro F.R., Sollima A., Pancino E., Bellazzini M., Straniero O., Origlia L., Cool A.M., 2004, *ApJ*, 603, 81

Ferraro F.R., Valenti E., Straniero O., Origlia L., 2006, *ApJ*, 642, 225

Fischer D.A., Valenti J., 2005, *ApJ*, 622, 1102

Fulbright J.P., 2000, *AJ*, 120, 1841

Fuhrmann K., 2004, *AN*, 325, 3

Gallart C., Zoccali M., Aparicio A., 2005, *ARA&A*, 43, 387

Gehren T., Butler K., Mashonkina L., Reetz J., Shi J., 2001a, 366, 981

Gehren T., Korn A.J., Shi J., 2001b, *A&A*, 380, 645

Gilli G., Israelian G., Ecuivillon A., Santos N.C., Mayor M., 2006, *A&A*, 449, 723

Girardi L., Bressan A., Bertelli G., Chiosi C., 2000, *A&AS*, 141, 371

Girardi L., Castelli F., Bertelli G., Nasi E., 2007, preprint([astro-ph/0703094](http://astro-ph/0703094))

Gliese W., Jahreiß H., 1991, *Catalogue of Nearby Stars*. 3rd edn, Astron. Rechen-Institut, Heidelberg

Gonzalez G., 1997, *MNRAS*, 285, 403

Gonzalez G., 1998, *A&A*, 334, 221

Gonzalez G., 2003, *Rev. Mod. Phys.*, 75, 101

Gonzalez G., 2006, *PASP*, 118, 1494

Gonzalez G., Laws C., Tyagi S., Reddy B.E., 2001, *AJ*, 121, 432

Gratton R.G., Fusi Pecci F., Carretta E., Clementini G., Corsi C.E., Lattanzi M., 1997, *ApJ*, 491, 749

Gratton R.G., Carretta E., Eriksson K., Gustafsson B., 1999, *A&A*, 350, 955

Gratton R.G. et al., 2001, *A&A*, 369, 87

Gratton R.G., Carretta E., Claudi R., Lucatello S., Barbieri M., 2003, *A&A*, 404, 187

Gratton R., Sneden C., Carretta E., 2004, *ARA&A*, 42, 385

Grevesse N., Noels A., 1993, *Phys. Scr. T*, 47, 133

Griffin R.F., 2004, *Obs.*, 124, 258

Guenther D.B., Demarque P., 1997, *ApJ*, 484, 937

Guenther D.B., Demarque P., 2000, *ApJ*, 531, 503

Gustafsson B., 1999, ed. I. Hybeny, S. Heap, & R. Cornett, *ASP Conf. Ser.*, 192, 91

Hall R.G.J., 1948, *AJ*, 54, 102

Hanson R.B., 1979, *MNRAS*, 186, 875

Haywood J.W., Hegyi D.J., Gudehus D.H., 1992, *ApJ*, 392, 172

Hegyi D., Curott D., 1970, *Phys. Rev. Lett.*, 24, 415

Heintz W.D., 1993, *AJ*, 105, 1188

Henry T.J., McCarthy D.W.J., 1993, *AJ*, 106, 773

Henry T.J., Soderblom D.R., Donahue R.A., Baliunas S.L., 1996, *AJ*, 111, 439

Henry T.J., Franz O.G., Wasserman L.H., Benedict G.F., Shelus P.J., Ianna P.H., Kirkpatrick J.D., McCarthy D.W.J., 1999, *ApJ*, 512, 864

Henry G.W., Fekel F.C., Sowell J.R., Gearhart J.S., 2006, *AJ*, 132, 2489

Holmberg J., Flynn C., Portinari L., 2006, *MNRAS*, 367, 449

Izotov Y.I., Thuan T.X., Stasinska G., 2007, preprint(astro-ph/0702072)

Jimenez R., MacDonal J., 1996, *MNRAS*, 283, 721

Jimenez R., Thejll P., Jorgensen U.G., MacDonald J., Pagel B., 1996, *MNRAS*, 282, 926

Jimenez R., Flynn C., Kotoneva E., 1998, *MNRAS*, 299, 515

Jimenez R., Loeb A., 2002, *ApJ*, 573, 37

Jimenez R., Flynn C., MacDonald J., Gibson B.K., 2003, *Sci*, 299, 1552

Kaviraj S., Sohn S.T., O'Connell R.W., Yoon S.-J., Lee Y.W., Yi S.K., 2007, preprint(astro-ph/0703198)

Kervella P., Thévenin F., Di Folco E., Ségransan D., 2004, *A&A*, 426, 297

Kjeldsen H. et al., 2005, *ApJ*, 635, 1281

Korn A.J., Shi J., Gehren T., 2003, *A&A*, 407, 691

Kotoneva E., Flynn C., Chiappini C., Matteucci F., 2002, *MNRAS*, 336, 879

Kroupa P., Tout C.A., Gilmore G., 1993, *MNRAS*, 262, 545

Lacy C.H.S., Torres G., Claret A., Vaz L.P.R., 2005, *AJ*, 130, 2838

Lastennet E., Fernandes J., Valls-Gabaud D., Oblak E., 2003, *A&A*, 409, 611

Lebreton Y., Perrin M-N., Cayrel R., Baglin A., Fernandes J., 1999, *A&A*, 350, 587

Lebreton Y., 2000, *ARA&A*, 38, 35

Lebreton Y., Fernandes J., Lejeune T., 2001, *A&A*, 374, 540

Luck R.E., Heiter U., 2006, *AJ*, 131, 3069

Ludwig H.-G., Freytag B., Steffen M., 1999, *A&A*, 346, 111

Lee Y.-W., Joo J.-M., Sohn Y.-J., Rey S.-C., Lee H.-C., Walker A.R., 1999, *Nat*, 402, 55

Lutz T.E., Kelker D.H., 1973, *PASP*, 85, 573

Maeder A., 1992, *A&A* 264, 105

Maeder A., 1993, *A&A* 268, 833

McCarthy D.J. et al., 1993, *AJ*, 105, 652

Mermilliod J.-C., Mermilliod M., Hauck B., 1997, *A&AS*, 124, 349

Michaud G., Vauclair G., Vauclair S., 1983, *ApJ*, 267, 256

Miglio A., Montalbán J., 2005, *A&A*, 441, 615

Mishenina T.V., Soubiran C., Kovtyukh V.V., Korotin S.A., 2004, *A&A*, 418, 551

Moehler S., Sweigart A. V., Landsman W. B., Heber U., Catelan M., 1999, *A&A*, 346, 1

Morel P., Baglin A., 1999, *A&A*, 345, 156

Morel P., Thévenin F., 2002, *A&A*, 390, 611

Morel P., Morel C., Provost J., Berthomieu G., 2000a, *A&A*, 354, 636

Morel P., Provost J., Lebreton Y., Thévenin F., Berthomieu G., 2000b, *A&A*, 363, 675

Neuforge C., 1993, *A&A*, 268, 650

Noels A., Grevesse N., Magain P., Neuforge C., Baglin A., Lebreton Y., 1991, *A&A*, 247, 91

Norris J.E., 2004, *ApJ*, 612, 25

Pagel B.E.J., Portinari L., 1998, *MNRAS*, 298, 747

Palmieri R., Piotto G., Saviane I., Girardi L., Castellani V., 2002, *A&A*, 392, 115

Pancino E., Ferraro F.R., Bellazzini M., Piotto G., Zoccali M., 2000, *ApJ*, 534, 83

Pancino E., Pasquini L., Hill V., Ferraro F.R., Bellazzini M., 2002, *ApJ*, 568, 101

Pasinetti Fracassini L.E., Pastori L., Covino S., Pozzi A., 2001, *A&A*, 367, 521

Paulson D.B., Sneden C., Cochran W.D., 2003, *AJ*, 125, 3185

Peimbert M., Luridiana V., Peimbert A., 2007, preprint(astro-ph/0701580)

Perrin M.-N., de Strobel G.C., Cayrel R., Hejlesen P.M., 1977, *A&A*, 54, 779

Perryman M.A.C. et al., 1998, *A&A*, 331, 81

Peterson R.C., Carney B.W., 1979, *ApJ*, 231, 762

Petit P. et al., 2005, *MNRAS*, 361, 837

Pinsonneault M.H., Deliyannis C.P., Demarque P., 1992, *ApJS*, 78, 179

Pinsonneault M.H., Walker T.P., Steigman G., Narayan V.K., 1999, *ApJ*, 527, 180

Pinsonneault M.H., Steigman G., Walker T.P., Narayan V.K., 2002, *ApJ*, 574, 398

Pinsonneault M.H., Terndrup D.H., Hanson R.B., Stauffer J.R., 2003, *ApJ*, 598, 588

Pinsonneault M.H., Terndrup D.H., Hanson R.B., Stauffer J.R., 2004, *ApJ*, 600, 946

Popper D.M., 1997, 114, 1195

Pourbaix D. et al., 2002, *A&A*, 386, 280

Ramírez I., Meléndez J., 2005, *ApJ*, 626, 465

Richard O., Michaud G., Richer J., Turcotte S., Turck-Chièze S., VandenBerg D.A., 2002, *ApJ*, 568, 979

Richard O., Michaud G., Richer J., 2005, *ApJ*, 619, 538

Rocha-Pinto H., Maciel W., 1998, *MNRAS*, 298, 332

Ryan S.G., Beers T.C., Deliyannis C.P., Thorburn J.A., 1996, *ApJ*, 458, 543

Ryan S.G., Norris J.E., Beers T.C., 1999, *ApJ*, 523, 654

Saffe C., Gómez M., Chavero C., 2005, *A&A*, 443, 609

Salaris M., Weiss A., 2001, *A&A*, 376, 955

Salaris M., Groenewegen M.A.T., Weiss A., 2000, *A&A*, 355, 299

Salaris M., Riello M., Cassisi S., Piotto G., 2004, *A&A*, 420, 911

Salasnich B., Girardi L., Weiss A., Chiosi C., 2000, *A&A*, 361, 1023

Sandage A., Saha A., 2002, AJ, 123, 2047  
 Sandquist E.L., 2000, MNRAS, 313, 571  
 Santos N.C., Israelian G., Mayor M., 2000, A&A, 363, 228  
 Santos N.C., Israelian G., Mayor M., 2004, A&A, 415, 1153  
 Santos N.C., Israelian G., García López R.J., Mayor M., Rebolo R., Randich S., Ecuivillon A., Domínguez Cerdeña C., 2004, A&A, 427, 1085  
 Santos N.C., Israelian G., Mayor M., Bento J.P., Almeida P.C., Sousa S.G., Ecuivillon A., 2005, A&A, 437, 1127  
 Schiller S.J., Milone E.F., 1987, AJ, 93, 1471  
 Schmitt J.H.M.M., Liefke C., 2004, A&A, 417, 651  
 Smith H.J., 1985, A&A, 152, 413  
 Smith H.J., 1987, A&A, 188, 233  
 Smith H., 2003, MNRAS, 338, 891  
 Smith H.J., Eichhorn H., 1996, MNRAS, 281, 211  
 Spergel D.N. et al., 2006, preprint(astro-ph/0603449)  
 Spite F., Spite M., 1982, A&A, 115, 357  
 Straniero O., Chieffi A., Limongi M., 1997, ApJ, 490, 425  
 Söderhjelm S., 1999, A&A, 341, 121  
 ten Brummelaar T.A., Mason B.D., McAlister H.A., Roberts L.C.J., Turner N.H., Hartkopf W.I., Bagnuolo W.G.J., 2000, AJ, 119, 2403  
 Thévenin F., Idiart T.P., 1999, ApJ, 521, 753  
 Thévenin F., Provost J., Morel P., Berthomieu G., Bouchy F., Carrier F., 2002, A&A, 392, 9  
 Thorburn J.A., 1994, ApJ, 421, 318  
 Torres G., Ribas I., 2002, ApJ, 567, 1140  
 Torres G., Boden A., Latham D.W., Pan M., Stefanik R.P., 2002, AJ, 124, 1716  
 Torres G., Lacy C.H., Marschall L.A., Sheets H.A., Mader J.A., 2006, ApJ, 640, 1018  
 Trampedach R., Stein R.F., Christensen-Dalsgaard J., Nordlund Å., 1999, in Gimenez A., Guinan E.F., Montesinos B., eds, ASP Conf. Ser. Vol. 173, Theory and Tests of Convection in Stellar Structure. Astron. Soc. Pac., San Francisco, p.233  
 Trotta R., Hansen S.H., 2004, Phys. Rev. D, 69, 023509  
 Underhill A.B., 1963, Pub. Dominion Astrophys. Obs., 12, 159  
 Valenti J.A., Fischer D.A., 2005, ApJS, 159, 141  
 VandenBerg D.A., Bridges T.J., 1984, ApJ, 278, 679  
 Vauclair S., 1988, ApJ, 335, 971  
 Vauclair S., Charbonnel C., 1995, A&A, 295, 715  
 Weis E.W., 1983, PASP, 95, 29  
 Weis E.W., 1996, AJ, 112, 2300  
 Weiss A., Salaris M., 1999, A&A, 346, 897  
 Wood B.E., Linsky J.L., 2006, ApJ, 643, 444  
 Yıldız M., 2007, MNRAS, 374, 1264  
 Yıldız M., Yakut K., Bakış H., Noels A., 2006, MNRAS, 368, 1941

## APPENDIX A: THE LUTZ-KELKER BIAS

The Lutz-Kelker bias on the absolute magnitude is in principle present at any level of parallax accuracy. The bias has two components, the first of which is statistical: since the number of stars increases with decreasing parallaxes (i.e. larger distances and sampled volumes) observational errors on the parallax will not cancel out exactly, giving a net effect of more stars with overestimated parallaxes. This makes

the correction on the magnitudes of the individual stars statistical and dependent upon the properties of the sample. The second component of the bias arises because distances (and hence absolute magnitudes) are not linear functions of the parallaxes. Even if errors have a normal distribution in parallax, they propagate to a skewed distribution in distance (absolute magnitude). Once again the effect is to favor more distant (brighter) stars to appear closer (fainter). It is clear that this is a correction that has to be applied to the absolute magnitude of individual stars.

In recent literature there is a certain degree of confusion about what exactly is the Lutz-Kelker bias, whether any correction should be applied and, if so, how large it should be. The value of the corrections to be applied depends on the distribution of the true parallaxes  $\omega_0$ . In principle the true parallax distribution could be derived by deconvolving the observed distribution for observational errors. In practice, the deconvolution process is quite uncertain and most of the authors prefer to use analytical formulae for the correction. The most widely used is that of Hanson (1979), who gave analytical formulae relating absolute magnitude corrections to the proper motion distribution of the sample of stars. However, the use of such formulation is highly risky and it does not provide the necessary accuracy because of the strong dependence on the variety of input parameters. As recommended by Brown et al. (1997) in their paper on the properties of the *Hipparcos* catalog, any correction should be tailored for each specific case. In fact, the blind use of Hanson's formulation is often counterproductive as noticed already by many authors (Gratton et al. 1997, Sandage & Saha 2002). Assuming a uniform density case, Hanson's formulation can be used as an estimator for the worst-case scenario, but not as a correction for the bias. Since the *Hipparcos* catalog completeness decreases with increasing magnitude, the statistical correction is negligible.

On the other hand, since we are dealing with the magnitude difference between individual stars and a reference isochrone, the correction for the skewed distribution is more relevant (at least in principle). Since magnitudes (and distances) are not linear functions of the parallax, one needs to resort to likelihood methods where the complete probability distribution function (pdf) of  $\omega$  given its uncertainties, is transformed into the corresponding distribution function for distance and magnitude. By means of such a method we prove the bias to be well within our observational errors.

Assuming a Gaussian distribution for the errors around the measured parallax  $\omega$

$$f(\tilde{\omega}) = \frac{1}{\sqrt{2\pi}\sigma} e^{-\frac{(\tilde{\omega}-\omega)^2}{2\sigma^2}}, \quad (A1)$$

the expectation value for the distance  $R$  is

$$E[R|\omega] = \int_{-\infty}^{+\infty} \frac{1}{\tilde{\omega}} f(\tilde{\omega}) d\tilde{\omega} = \frac{1}{\sqrt{2\pi}\sigma} \int_{-\infty}^{+\infty} g(\tilde{\omega}) e^{\frac{t(\tilde{\omega})}{2\sigma^2}} d\tilde{\omega} \quad (A2)$$

where  $g(\tilde{\omega}) = 1/\tilde{\omega}$  and  $t(\tilde{\omega}) = -(\tilde{\omega}-\omega)^2$ . Defining  $u = \tilde{\omega}-\omega$  and expanding  $g(\tilde{\omega})$  around the maxima of  $t(\tilde{\omega})$  one gets the following series

$$g(\tilde{\omega}) = \frac{1}{\omega} \sum_{n=0}^{\infty} (-1)^n \left(\frac{u}{\omega}\right)^n. \quad (A3)$$

Given the accuracy of our parallaxes, the condition  $|u/\omega| < 1$  for the expansion is certainly satisfied within, say,  $3\sigma$ . The

choice of the  $3\sigma$  cutoff sounds perfectly reasonable for the purposes of our calculation. Alternatively, a more rigorous approach has been investigated by Smith & Eichhorn (1996).

Once the series expansion for  $g(\tilde{\omega})$  is known, the integral in eq. (A2) reads

$$E[R|\omega] = \frac{1}{\sqrt{2\pi}\sigma} \int_{-\infty}^{+\infty} \frac{1}{\omega} \sum_{n=0}^{\infty} (-1)^n \left(\frac{u}{\omega}\right)^n e^{-\frac{u^2}{2\sigma^2}} du \quad (\text{A4})$$

and can easily be calculated by using Gaussian integrals and noticing that odd terms vanish. The result is the following series

$$E[R|\omega] = \frac{1}{\omega} \sum_{n=0}^{\infty} \frac{(2n)!}{2^n n!} \left(\frac{\sigma}{\omega}\right)^{2n} \quad (\text{A5})$$

and the amplitude of the bias

$$E[R|\omega] - \frac{1}{\omega} \sim \frac{1}{\omega} \left(\frac{\sigma}{\omega}\right)^2 \quad (\text{A6})$$

can be easily checked to be negligible for our adopted accuracy in parallaxes (6%).

In the same manner we can give an estimate for the bias in absolute magnitudes  $M_\xi$  in a given band  $\xi$  or bolometric. We thus have

$$E[M_\xi|\omega] = \frac{1}{\sqrt{2\pi}\sigma} \int_{-\infty}^{+\infty} g(\tilde{\omega}) e^{\frac{t(\tilde{\omega})}{2\sigma^2}} d\tilde{\omega}, \quad (\text{A7})$$

where now, for a given apparent magnitude  $\xi$ , we have

$$g(\tilde{\omega}) = \xi + 5 \log(\tilde{\omega}) - 10. \quad (\text{A8})$$

Hence the integral to be computed is

$$E[M_\xi|\omega] = \frac{1}{\sqrt{2\pi}\sigma} \int_{-\infty}^{+\infty} \left[ \xi + 5 \log(\omega) - 10 + 5 \log(e) \sum_{n=1}^{\infty} \frac{(-1)^{n+1}}{n} \left(\frac{u}{\omega}\right)^n \right] e^{-\frac{u^2}{2\sigma^2}} du \quad (\text{A9})$$

and gives the following bias

$$E[M_\xi|\omega] - M_\xi = -5 \log(e) \sum_{n=1}^{\infty} \frac{(2n-1)!}{2^n n!} \left(\frac{\sigma}{\omega}\right)^{2n}. \quad (\text{A10})$$

Also for the absolute magnitudes the bias is negligible. At the first order the above equation gives

$$E[M_\xi|\omega] - M_\xi = -\frac{5}{2} \log(e) \left(\frac{\sigma}{\omega}\right)^2 \sim -0.004 \text{ mag} \quad (\text{A11})$$

in the case of lowest parallax accuracy and thus well within our observational errors.

We finally note that given the high precision of our parallaxes ( $\sigma/\omega \leq 0.06$ ) a fully Bayesian approach is not needed, also considering that it would require a priori assumptions on the parameter distributions. A Bayesian approach is indeed demanded for lower precision parallaxes and it has been extensively studied by Smith (1985; 1987; 2003) in his series of papers on the Lutz-Kelker bias.